Field Measurements of 2x2 MIMO Communications

Babak Daneshrad, Prof
Mike Fitz, Prof

UCLA EE Dept.
babak@ee.ucla.edu, fitz@ee.ucla.edu
www.mimo.ucla.edu

Overview

- Testbed Overview
- Loss Due to IQ mismatch & phase noise
- Measurement Results
- MIMO Decoder ASIC

MIMO OFDM Testbed Overview

Top Level Functional Diagram

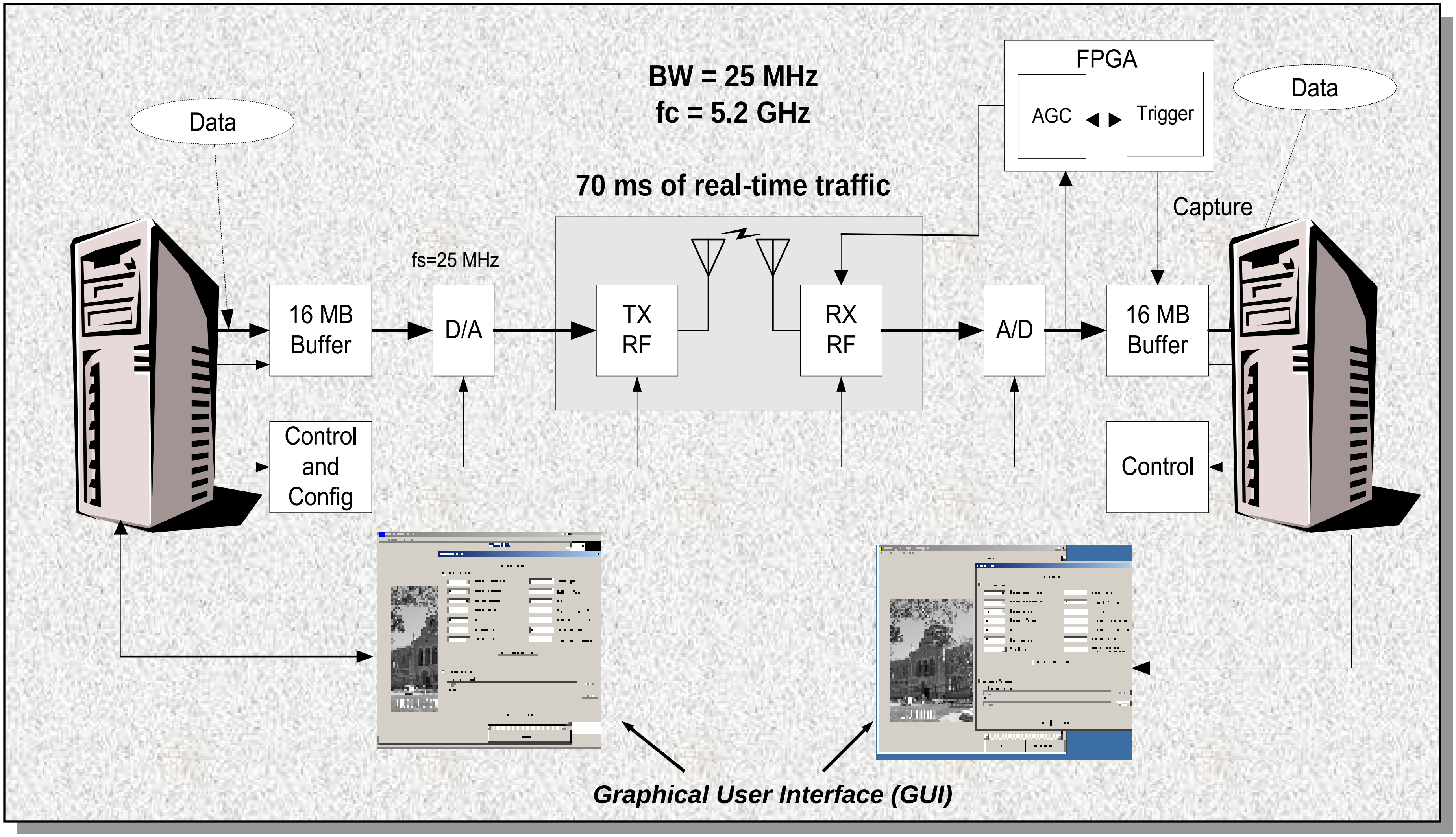

Testbed Components

UCLA Phase-2 2x2 MIMO Testbed

Memory Buffer
I/O Boards

PLX Control
Board

Phase Locked
Loop Circuit

Radio Freq.
Circuit

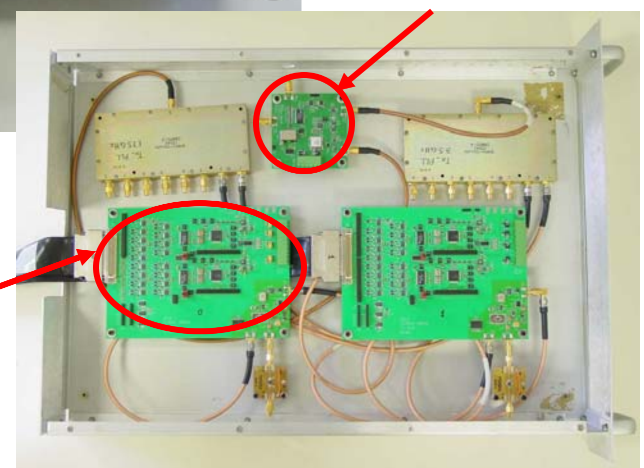

TX 2-Step RF Up-conversion

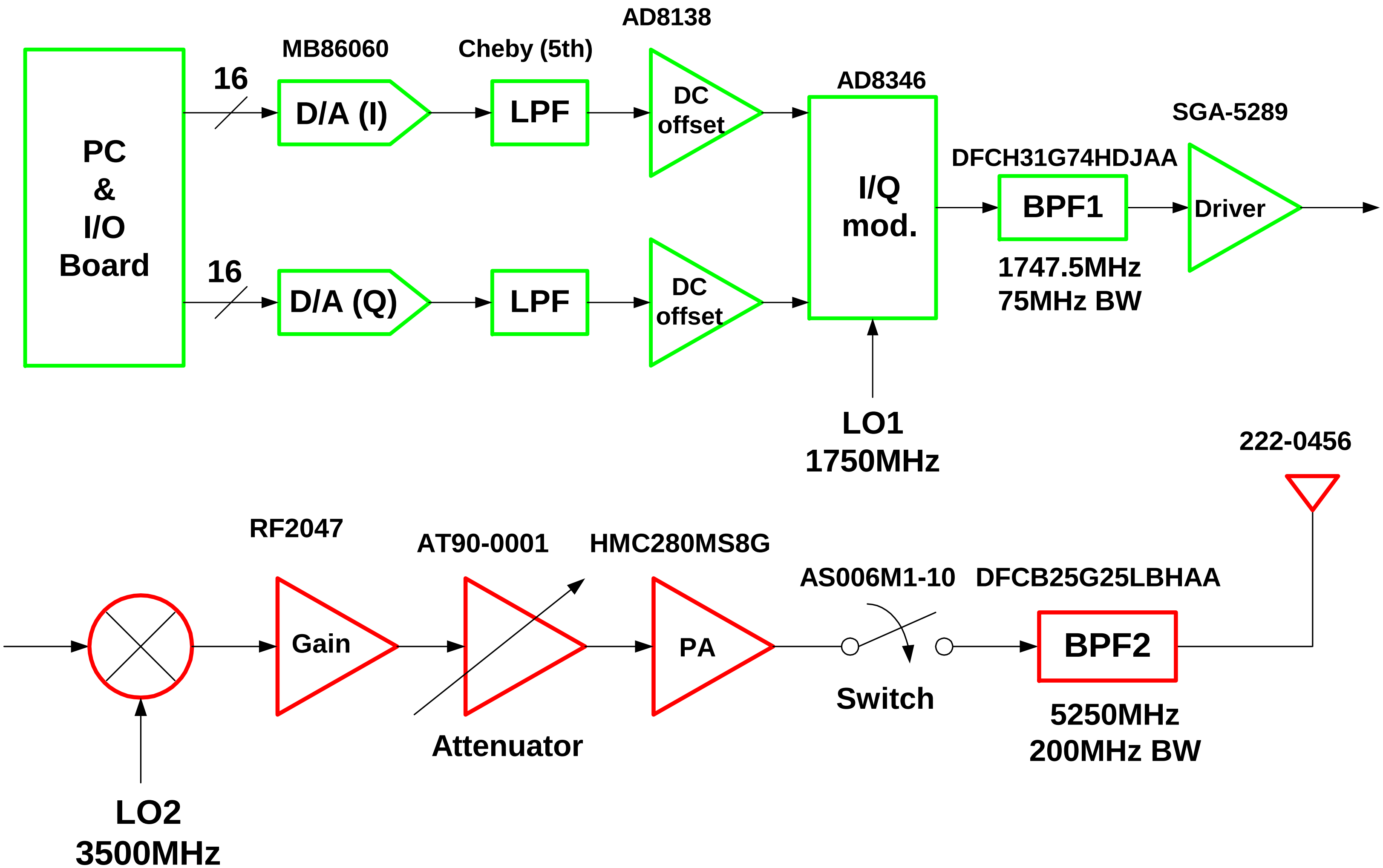

RX 2 step down-conversion

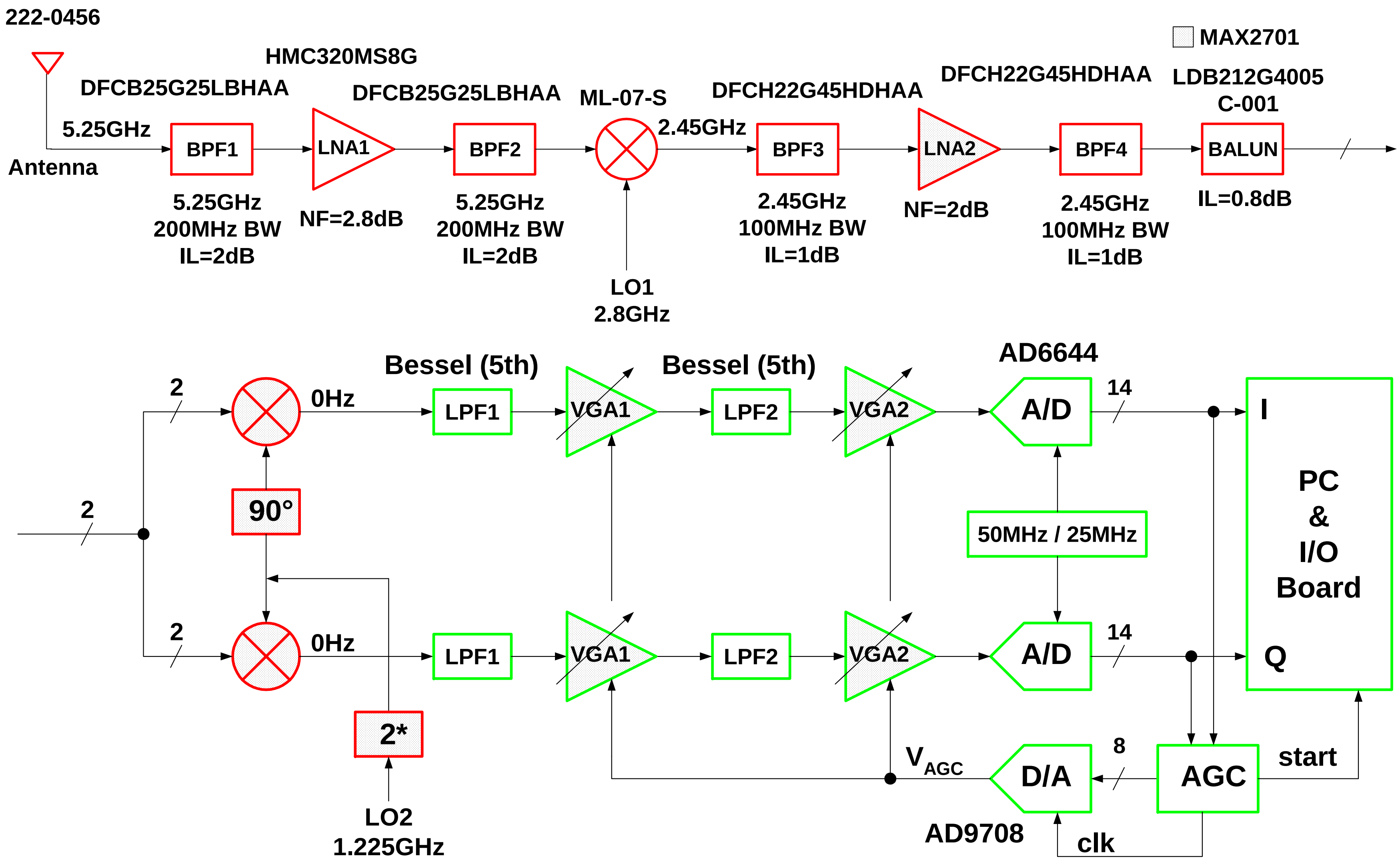

Packet Structure

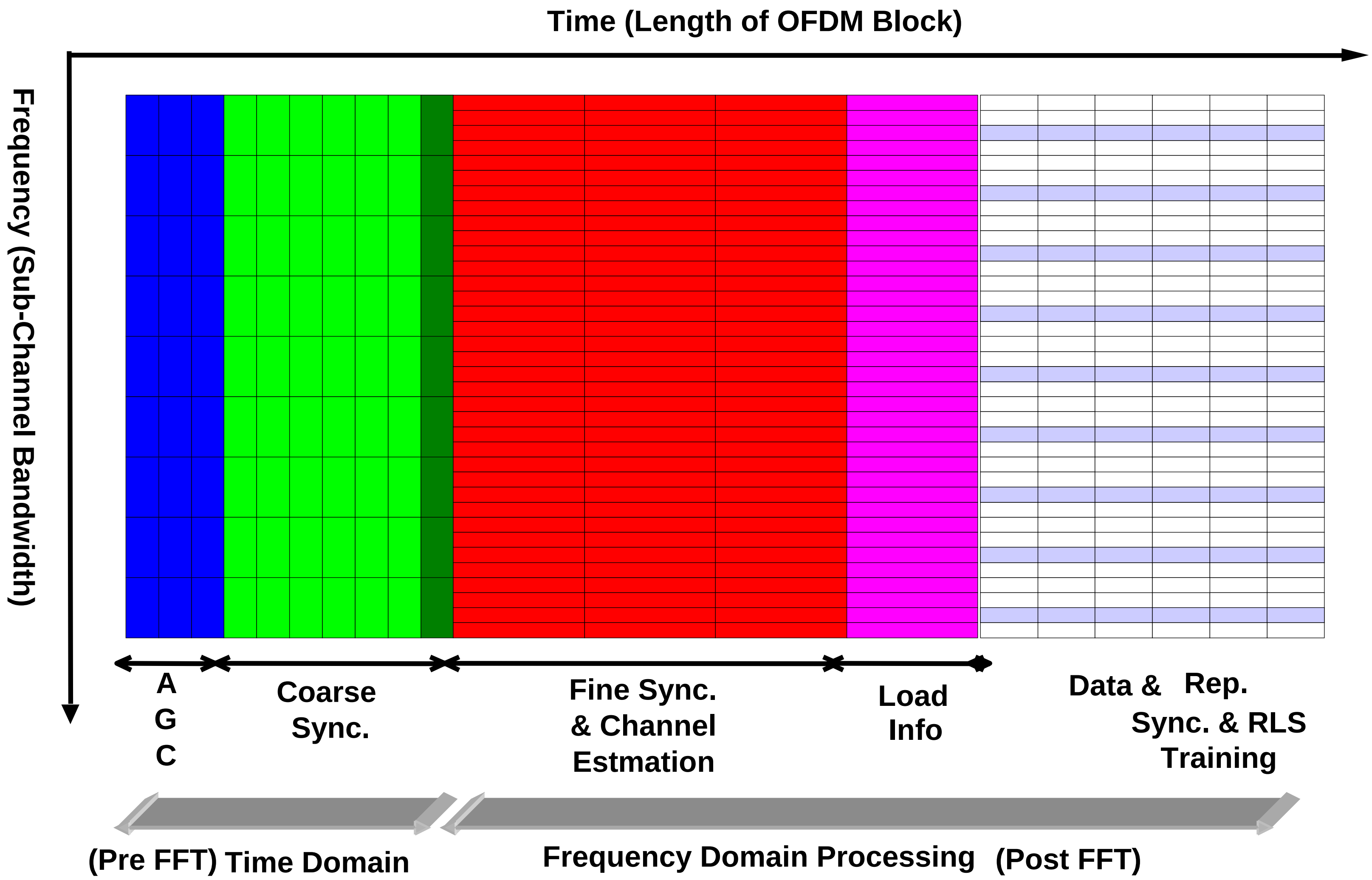

2 Major Impairments: Phase Noise & IQ Mismatch

- Phase noise mitigation is critical to OFDM

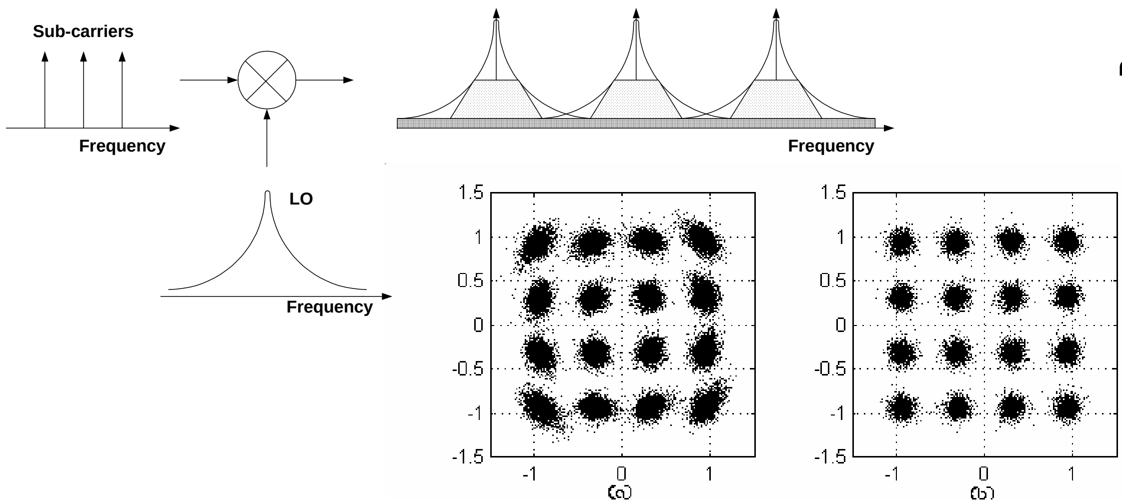

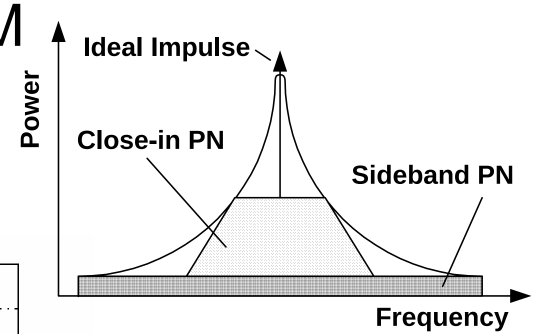

- IQ mismatch, gain and phase, is present in all practical RF circuits
  – I/Q mismatch causes interference subcarriers

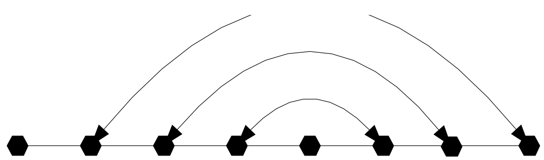

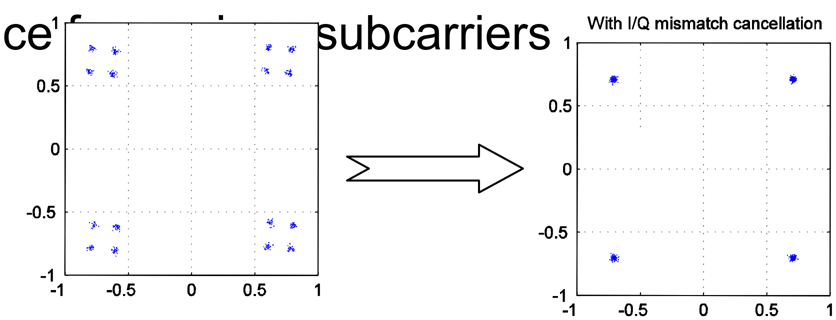

Calibration Metrics

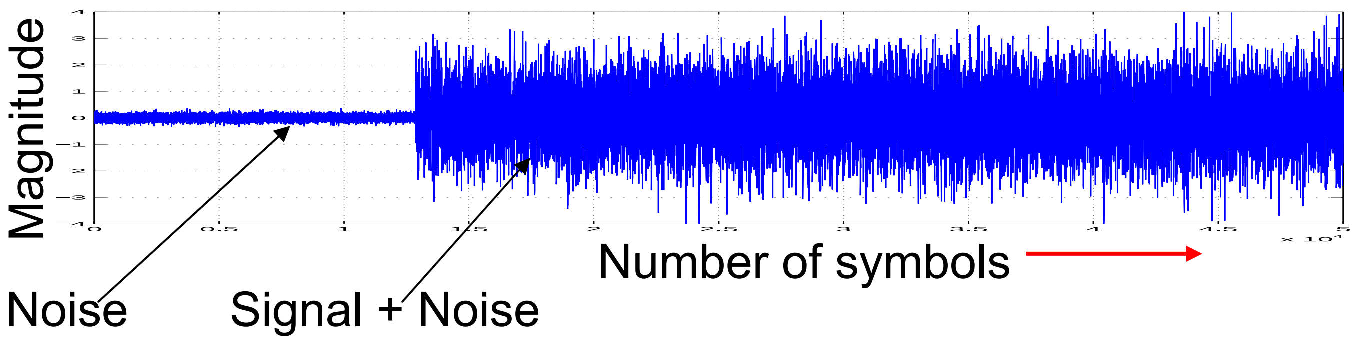

Calculated in the frequency domain

$$InputSNR = 10\log10(\frac{(Signal + Noise)\ Energy}{Noise\ Energy} - 1)$$

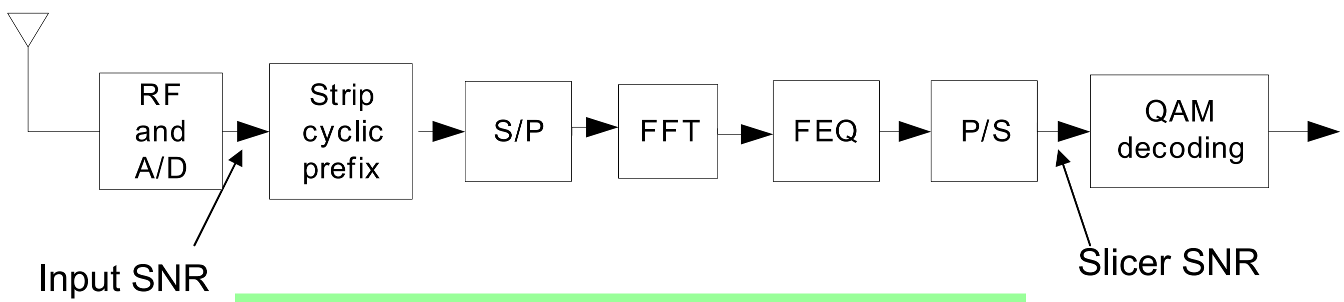

Implementation Loss = Input SNR-Slicer SNR

SER in Perfect Timing Mode

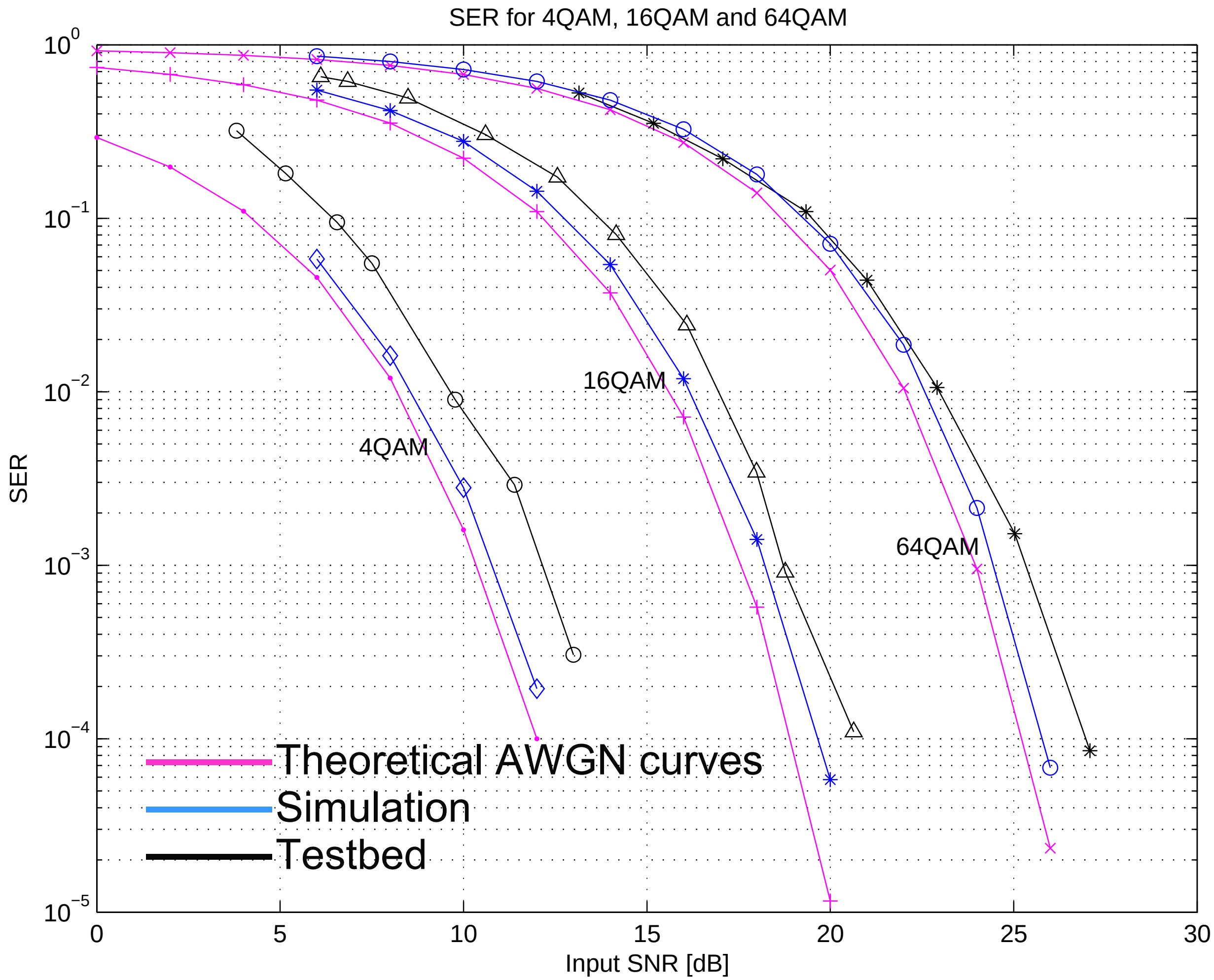

Testbed Calibration in Perfect Timing Mode

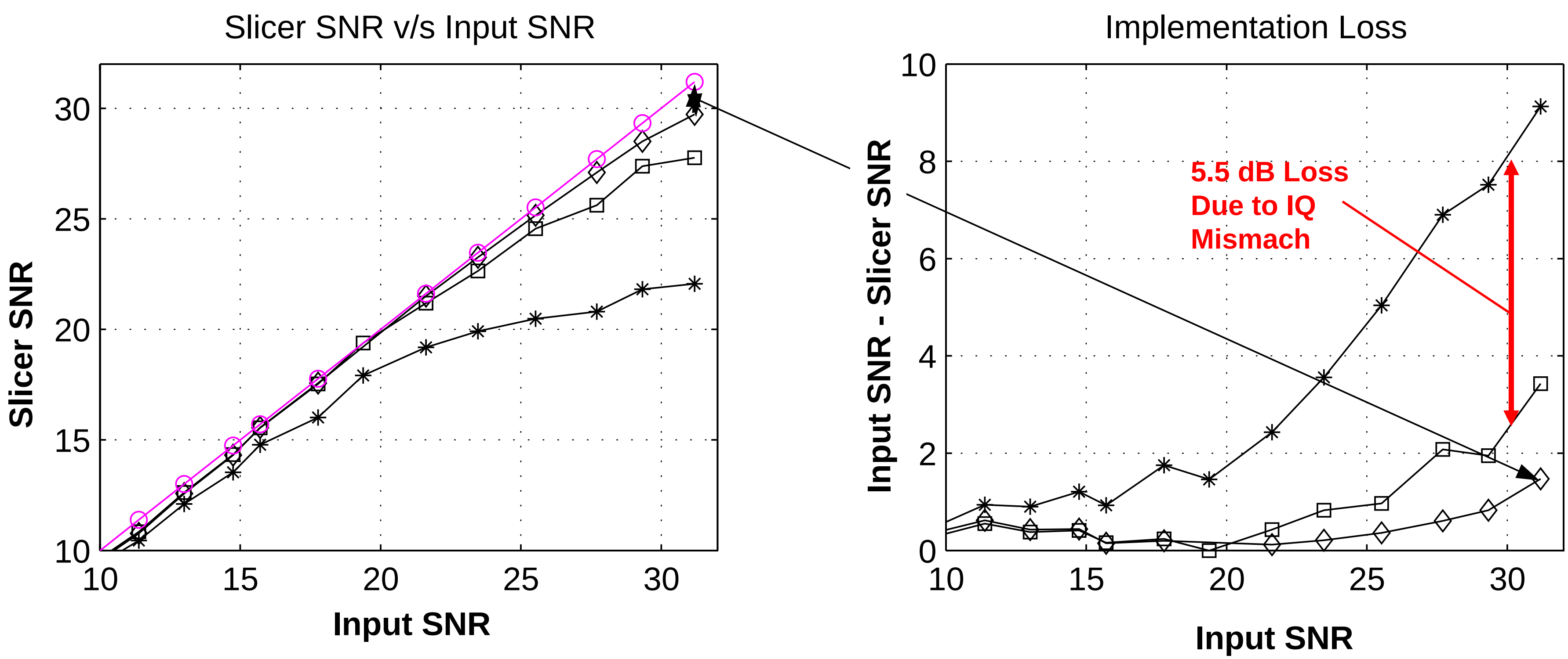

Comparing I/Q mismatch and Phase Noise Cancellation schemes on the testbed in perfect timing mode

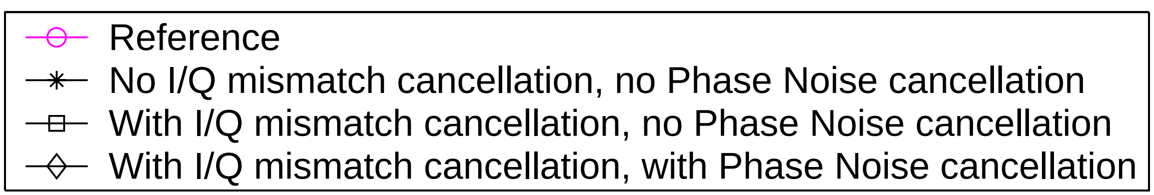

Implementation loss under non-perfect timing

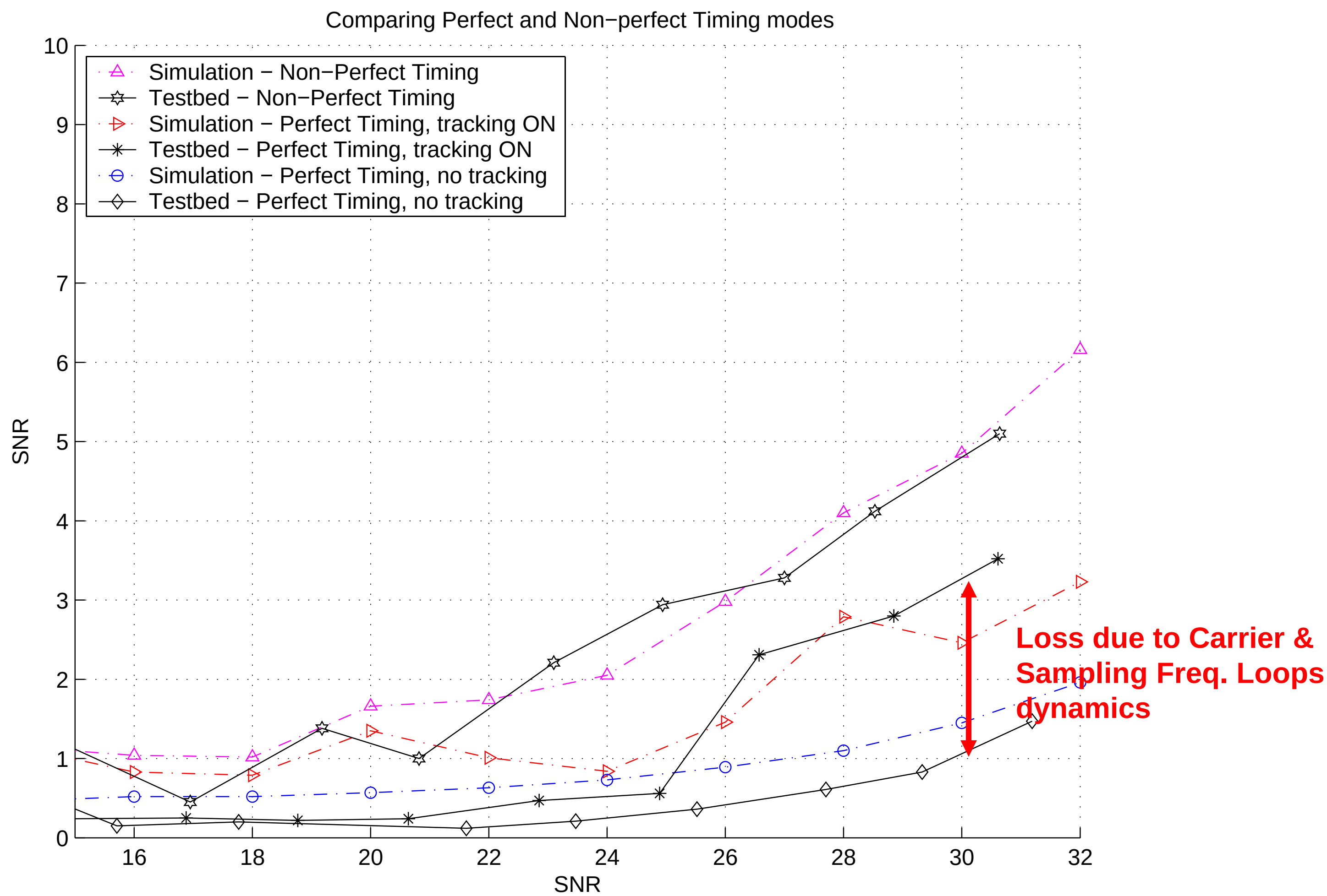

Simulated Performance of MIMO-OFDM with and w/o I/Q Mismatch Cancellation

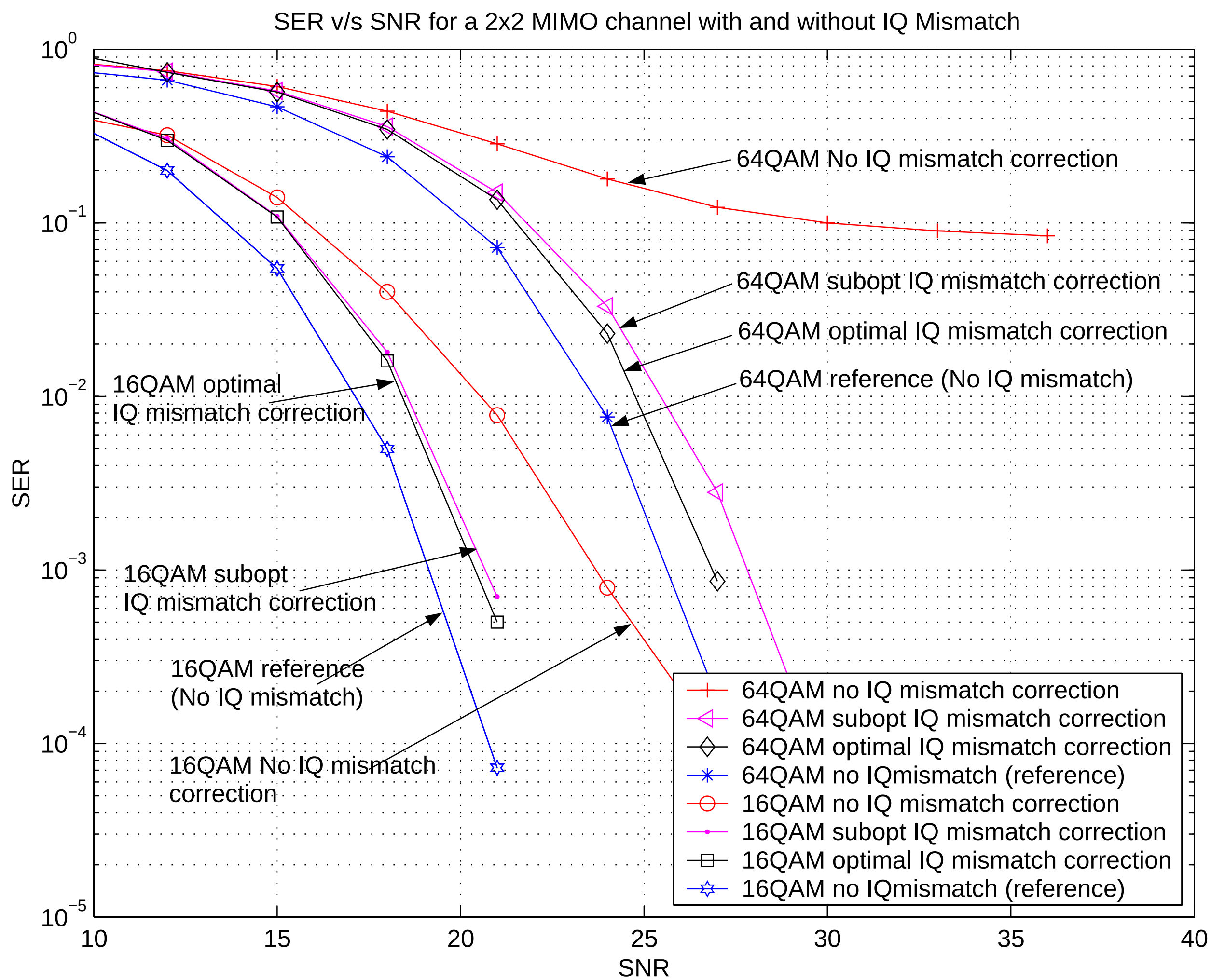

IQ gain mismatch
Tx1 - (0.75,0.90)
Tx2 - (0.85,0.95)
Rx1 - (0.85,1.00)
Rx2 - (0.90, 0.85)

IQ phase mismatch
6 degrees at both the receivers

MMSE IQ Mismatch Canceller

I/Q mismatch in MIMO-OFDM systems

- I/Q mismatch is caused by an imbalance on the I-rail and Q-rails. This imbalance could be gain, delay or phase.
  - Gain mismatch occurs when the amplifiers on I-rail and Q-rail have different gains.
  - Delay mismatch occurs when the propagation delays on the two rails are different due to trace mismatches, different D/A skews, etc.
  - Phase mismatch occurs when the sinusoids used in the I/Q modulators and demodulators are not offset by 90 degrees.
- I/Q mismatch can be categorized as frequency dependent or frequency dependent.
  - Gain and phase mismatches cause frequency independent I/Q mismatch.
  - Delay causes frequency dependent I/Q mismatch with distortion increasing on the high frequency subcarriers.

Effect of I/Q mismatch in an OFDM system

I/Q mismatch causes interference from the conjugate of the data on the frequency mirror sub-carrier.

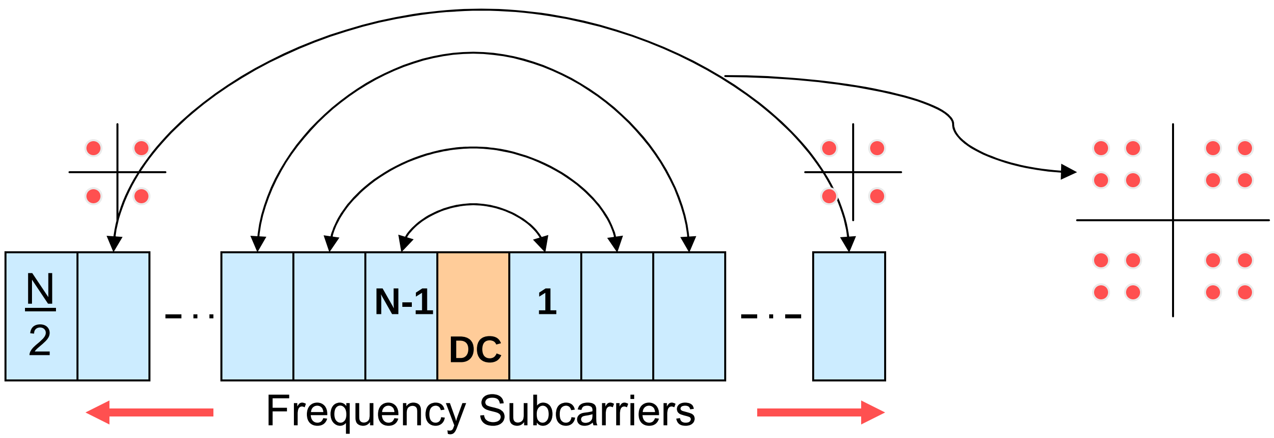

$$\tilde{Y}(k) = \left[\frac{A(k)+B(k)}{2}\right]X(k) + \left[\frac{A(k)-B(k)}{2}\right]X^*(N-k)$$

I/Q delay mismatch

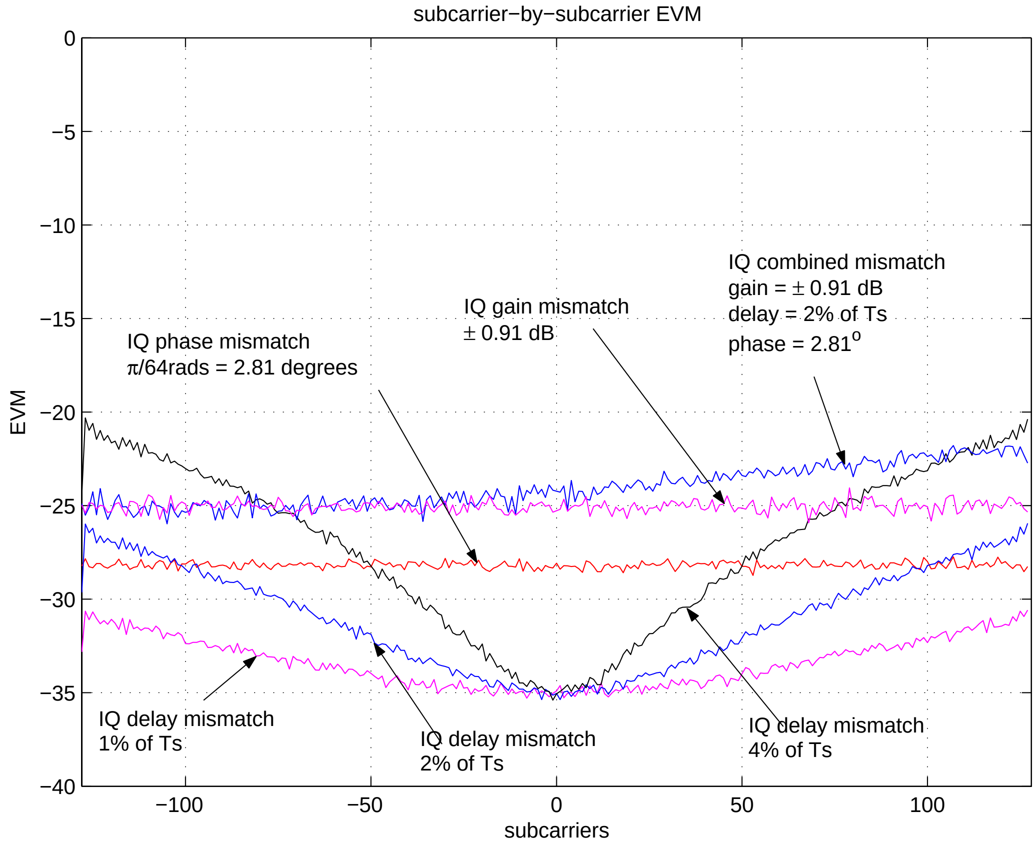

Image suppression

IQ mismatch	Min	Average
1% of Ts	-37.2 dB	-41.5 dB
2% of Ts	-31.3 dB	-35.5 dB
4% of Ts	-25.3 dB	-29.4 dB
2.81° phase	-32.19 dB	-32.19 dB
0.91dB gain	-25.57 dB	-25.57 dB

Image suppression is measured by transmitting data on half the subcarriers and measuring the image strength on the mirror frequencies

Effect of I/Q mismatch on a 4-QAM Constellation

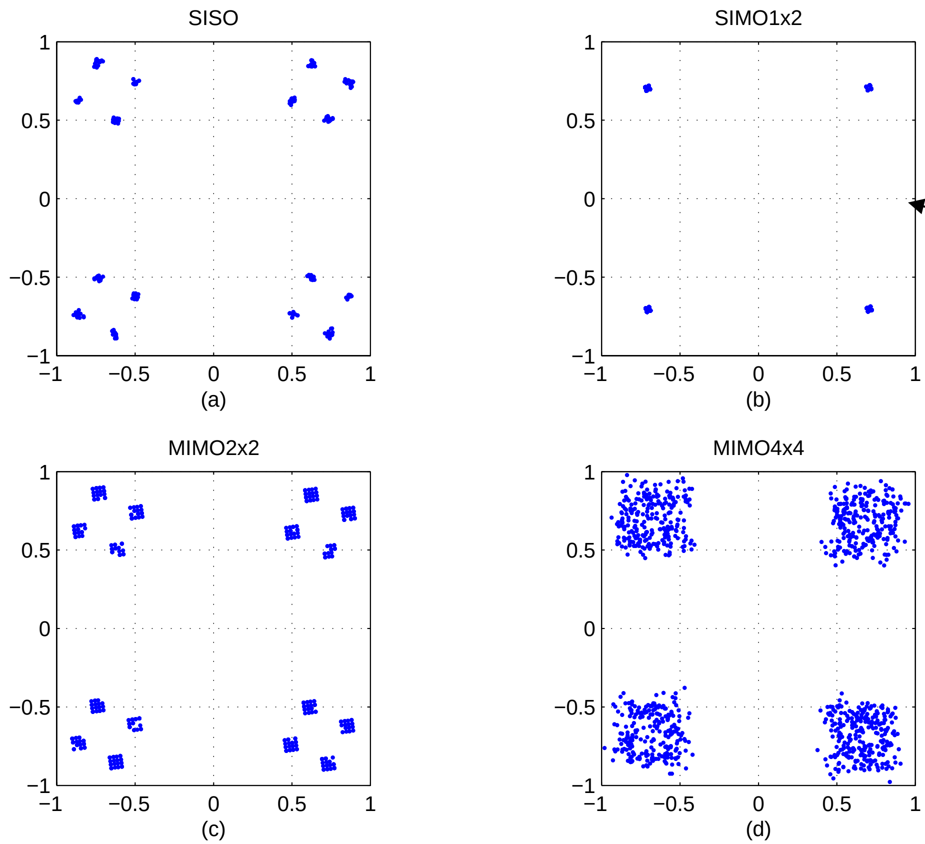

Receive diversity helps with IQ mismatch. SIMO1x2 shows good improvement without any I/Q mismatch cancellation algorithms

Image Suppression on the Testbed

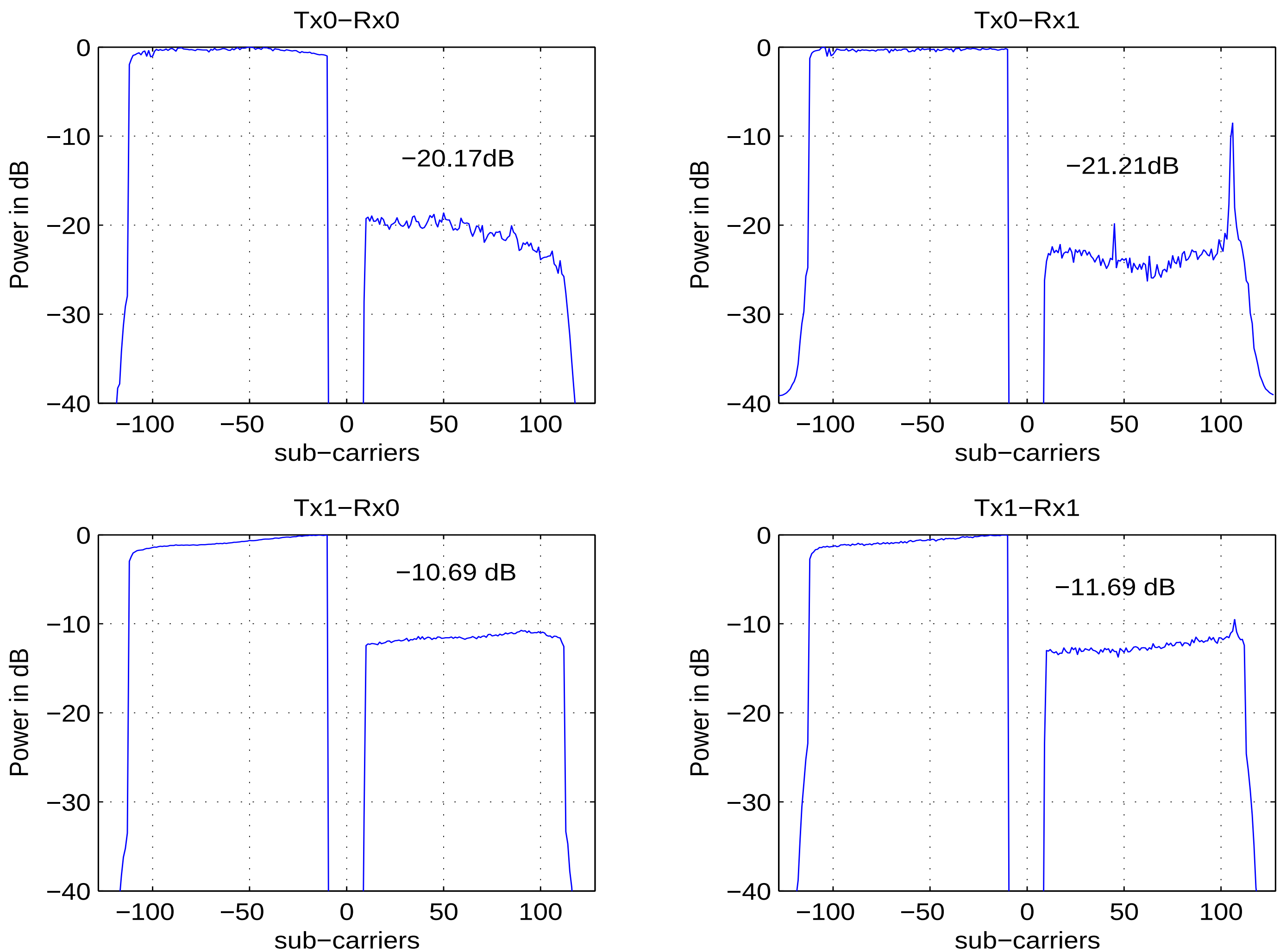

I/Q mismatch for MIMO-OFDM

For MIMO-OFDM there is interference from the conjugate of the data on the frequency mirror subcarrier of all the datastreams.

$$\begin{bmatrix} Y_1(k) \\ Y_2(k) \\ Y_1^*(N-k) \\ Y_2^*(N-k) \end{bmatrix} = \begin{bmatrix} P_1 & Q_1 & R_1 & S_1 \\ P_2 & Q_2 & R_2 & S_2 \\ P_3 & Q_3 & R_3 & S_3 \\ P_4 & Q_4 & R_4 & S_4 \end{bmatrix} \begin{bmatrix} X_1(k) \\ X_2(k) \\ X_1^*(N-k) \\ X_2^*(N-k) \end{bmatrix} + \begin{bmatrix} V_1(k) \\ V_2(k) \\ V_1^*(N-k) \\ V_2^*(N-k) \end{bmatrix}$$

I/Q mismatch and EDOF

- EDOF measured at 10% outage and 30dB SNR. Capacity at 10% outage, 30dB SNR

Image Suppression	-7.7dB		-10.79dB		-15.06dB		-21dB	
	EDOF	Cap.	EDOF	Cap.	EDOF	Cap.	EDOF	Cap.
1x1	0.95	9.7	0.96	10.35	0.97	10.68	0.98	11.3
2x2	1.84	21.05	1.87	22.50	1.89	23.82	1.9	25.02
2x4	1.981	28.25	1.987	30.00	1.990	31.51	1.992	32.83
4x4	3.662	45.69	3.733	48.56	3.765	51.19	3.787	53.55
8x8	7.39	93.96	7.495	99.82	7.576	105.07	7.588	109.88

- EDOF degrades slightly due to IQ mismatch !!
  - EDOF calculations use input SNR and channel estimates

$$C = \log_2(\det(I_M + \frac{\rho_R}{M} H^H H)) = \sum_{k=1}^{R} \log_2(1 + \frac{\rho_R}{M} \varepsilon_k^2) bits/s/Hz$$

A practical definition of EDOF is the difference in capacity when ρ_R is doubled.
EDOF=C($2\rho_R$)-C(ρ_R)
EDOF ranges from 0 to R

I/Q Mismatch Cancellation on the Testbed

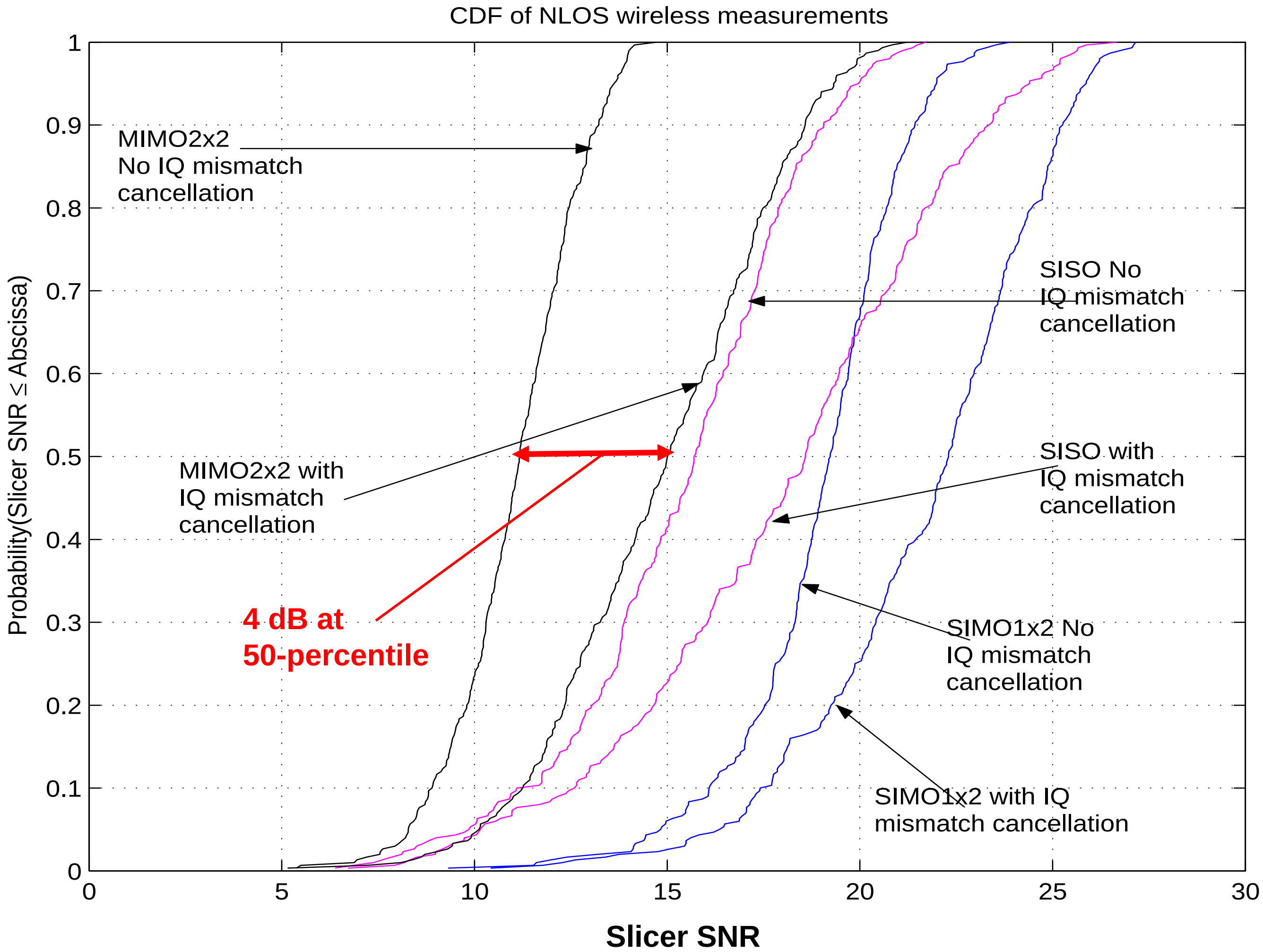

Phase Noise

Phase Noise PSD

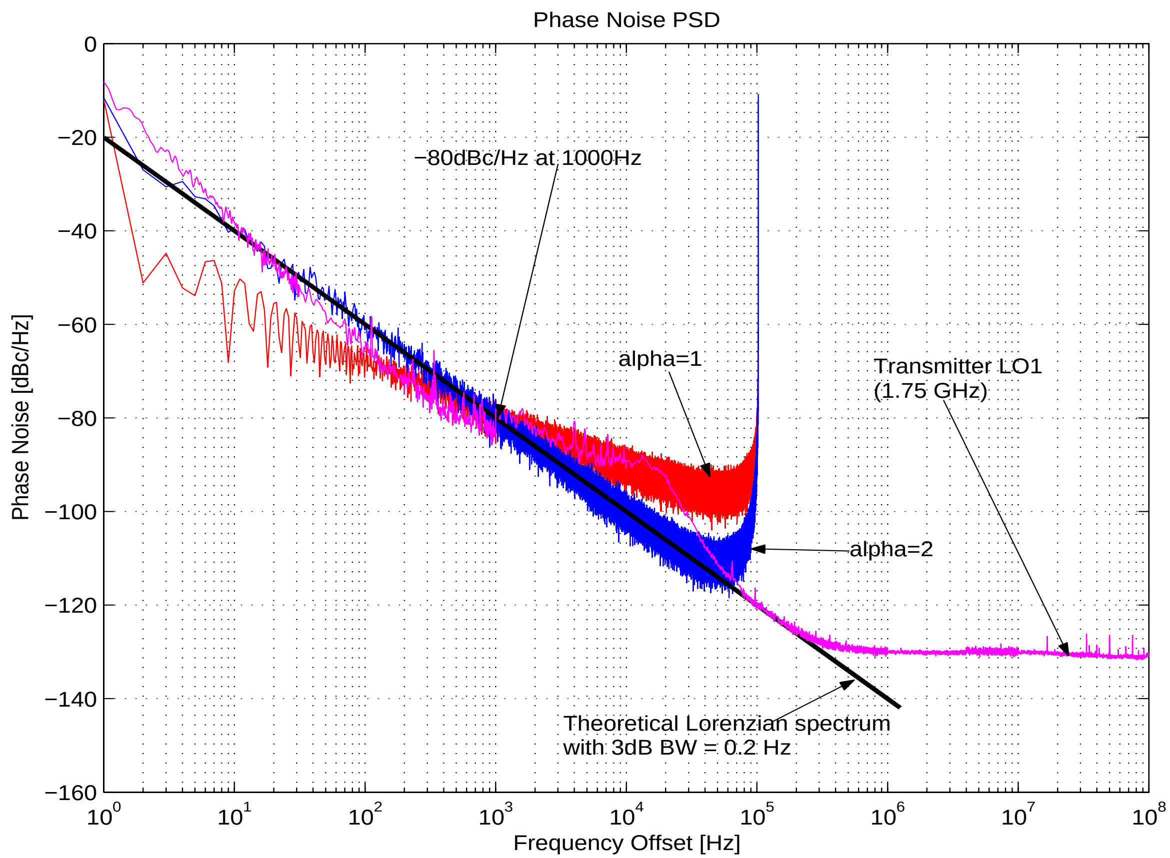

- For modeling use 1/f model, not $1/f^2$

Phase Noise with Varying FFT Sizes

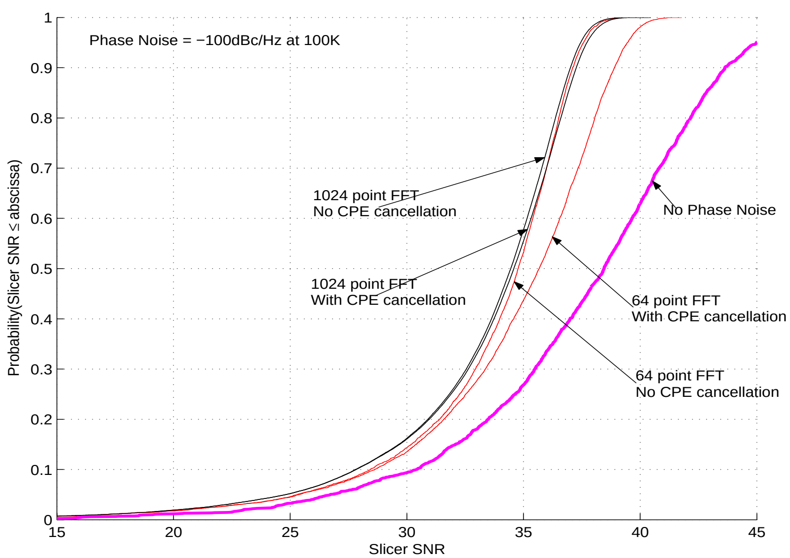

Compare FFT sizes

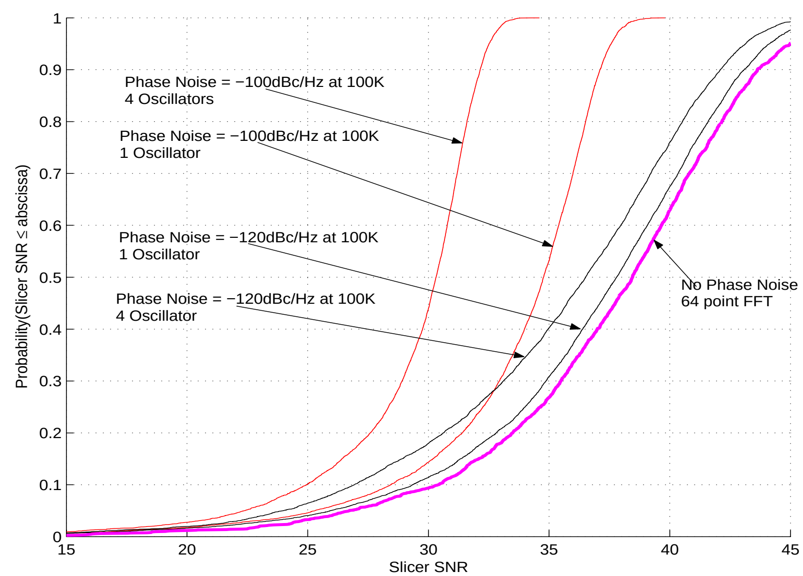

Compare 1 osc and 4 osc

- Common phase error (CPE) decreases with increasing FFT Size
  - More difficult to eliminate with CPE cancellation
  - 1.25 dB improvement with CPE cancellation when using 64 subcarrier SISO system
- CPE decreases with increasing MIMO configuartion
  - 0.75 dB to 1 dB with 2x2 64-point FFT

Experimental Measurements

Environment 1: Cubicle Area

τ_{rms} = 38 ns to 50 ns

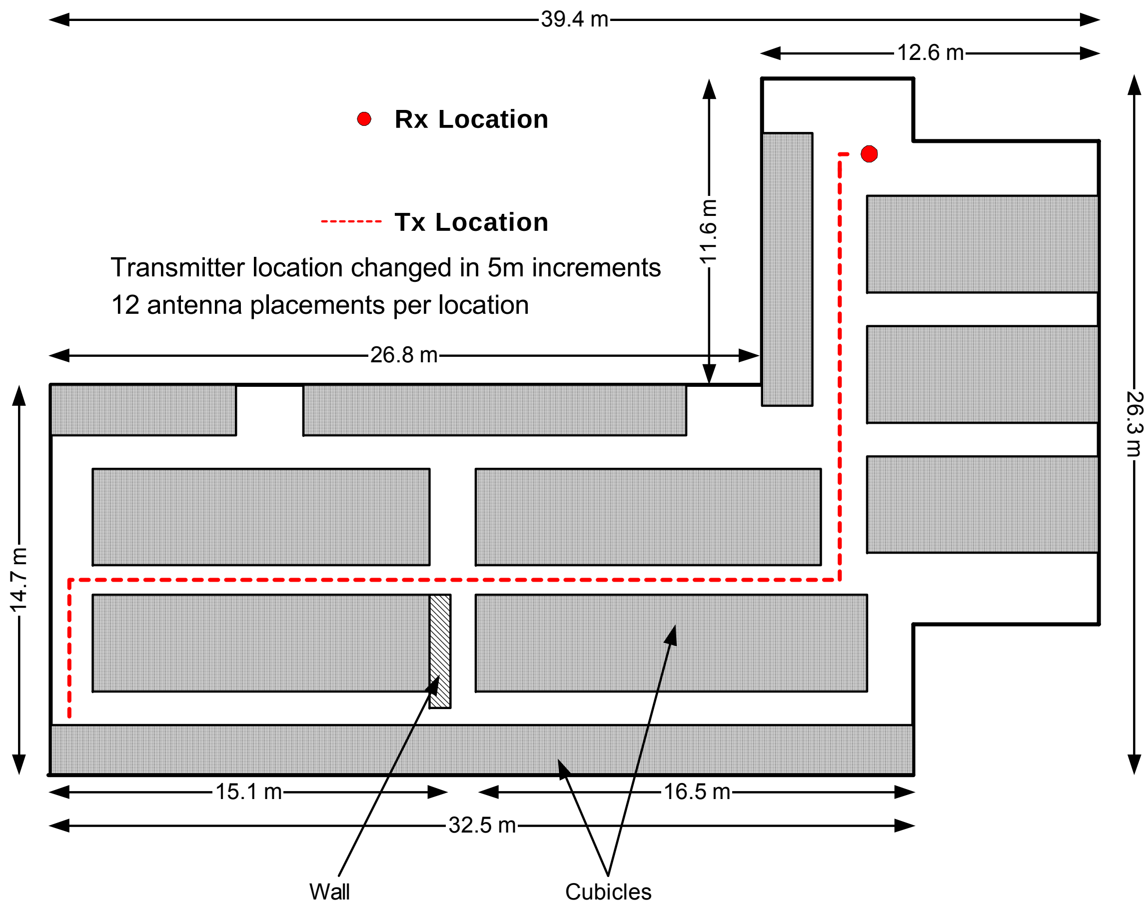

Range measurements in the cubicle area

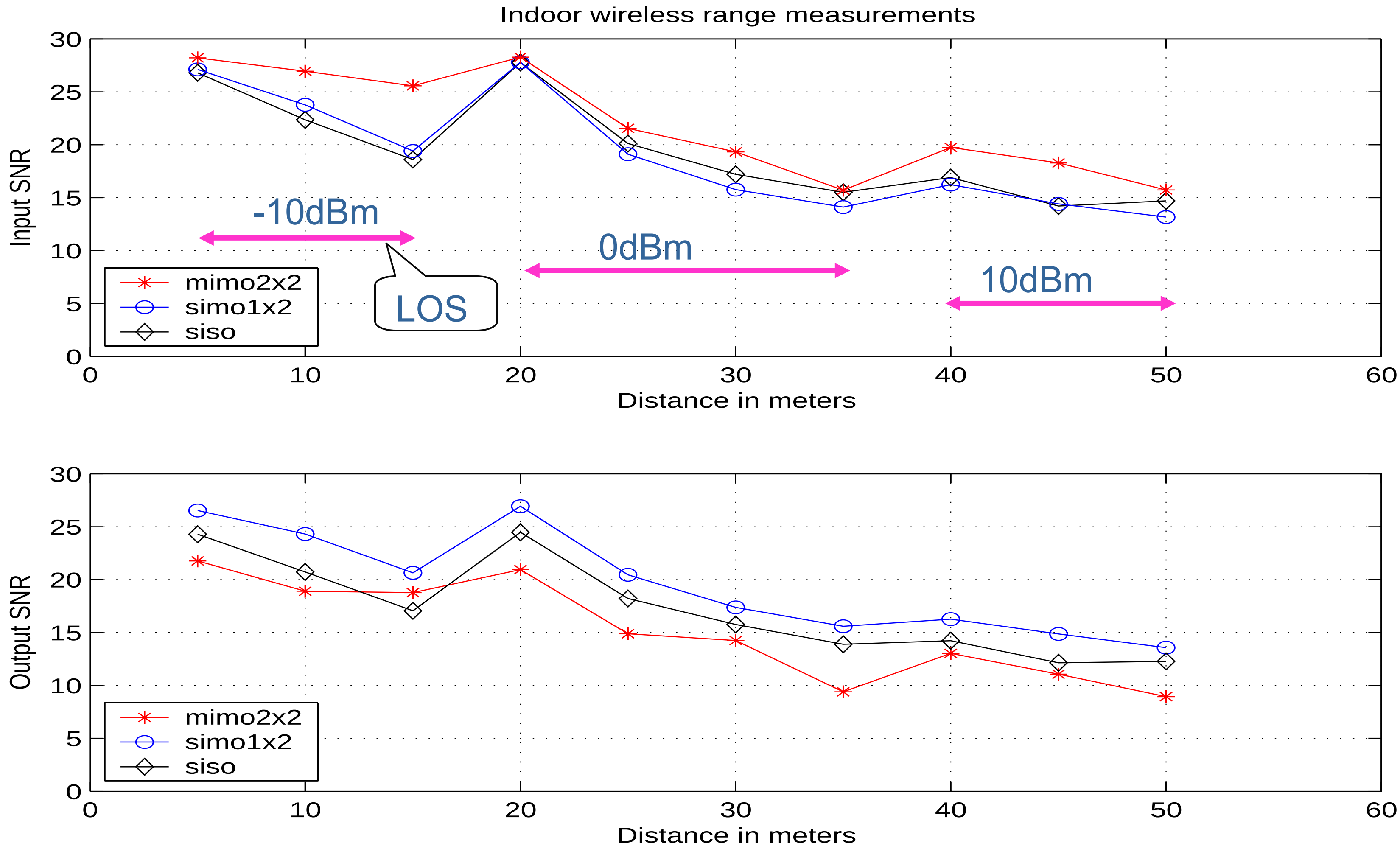

Controlled Field Trials

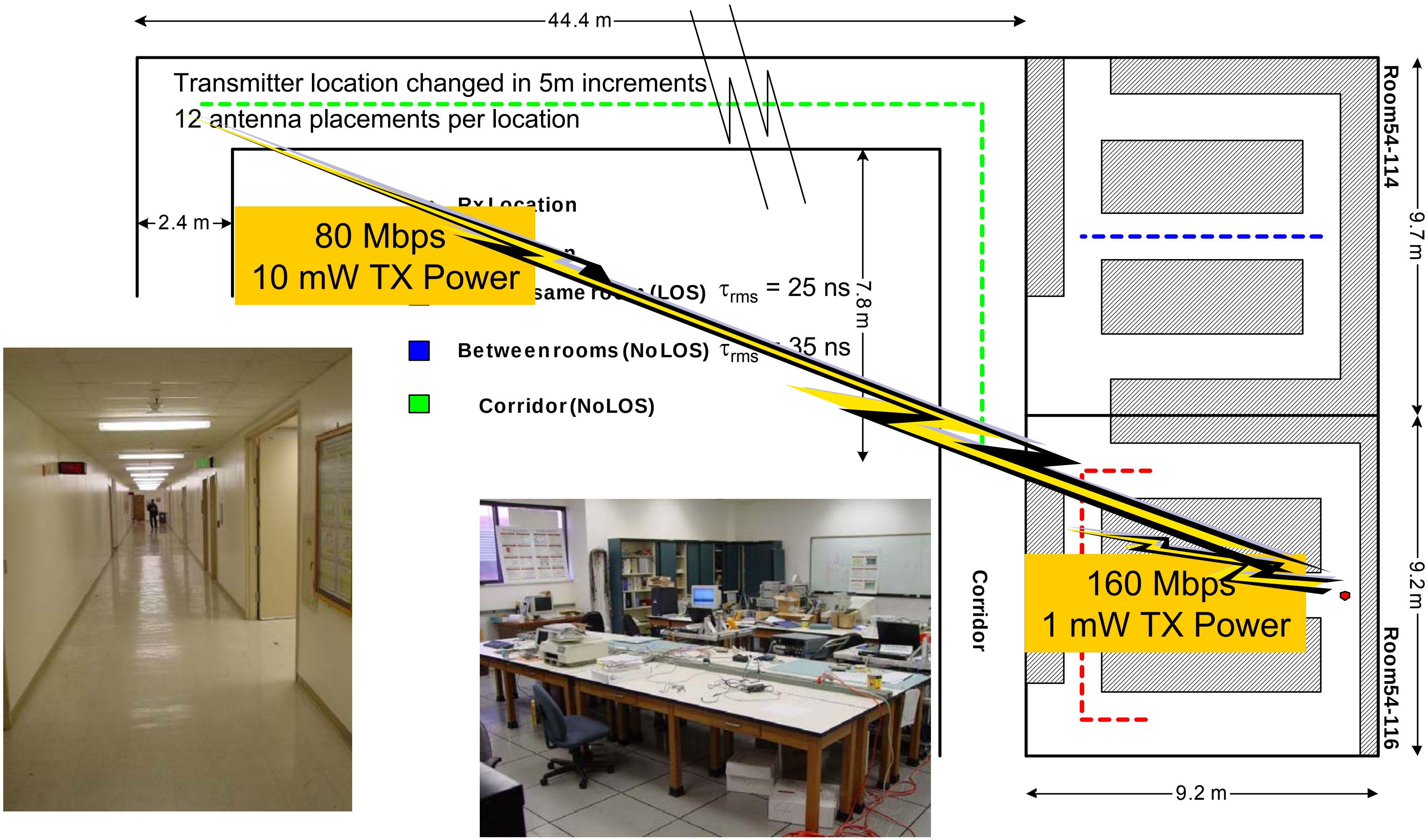

CDF of Slicer SNR for MIMO2x2, SIMO1x2 and SISO

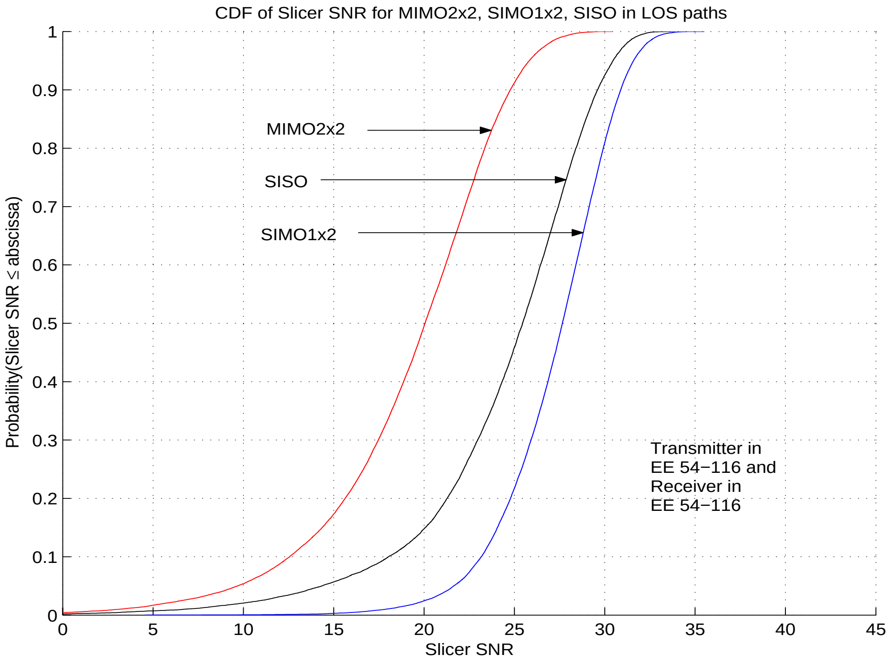

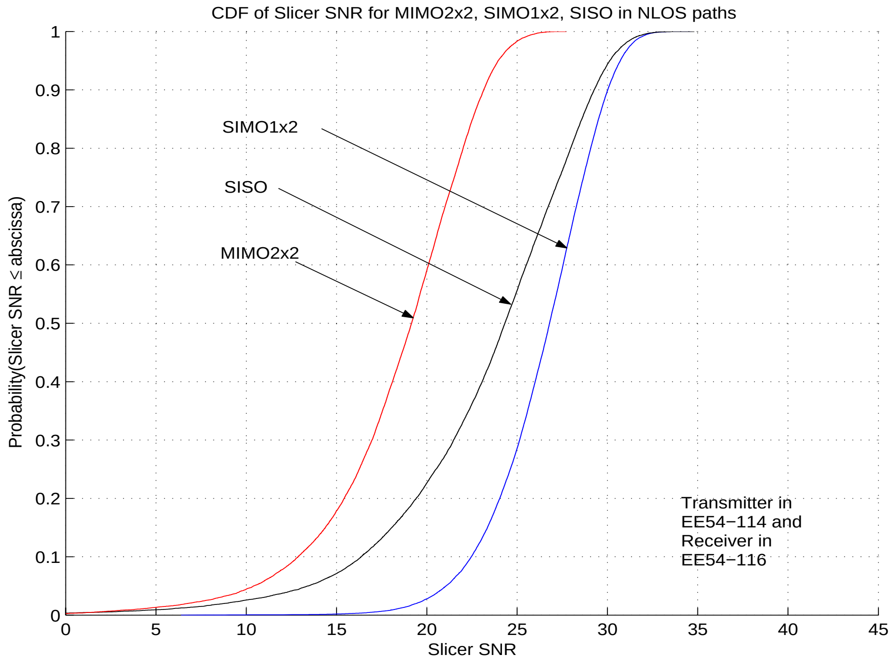

Reciprocal condition numbers

Information theoretic Capacity

$$C = \log_2(\det(I_M + \frac{\rho_R}{M} H^H H)) = \sum_{k=1}^{R} \log_2(1 + \frac{\rho_R}{M} \varepsilon_k^2) bits/s/Hz$$

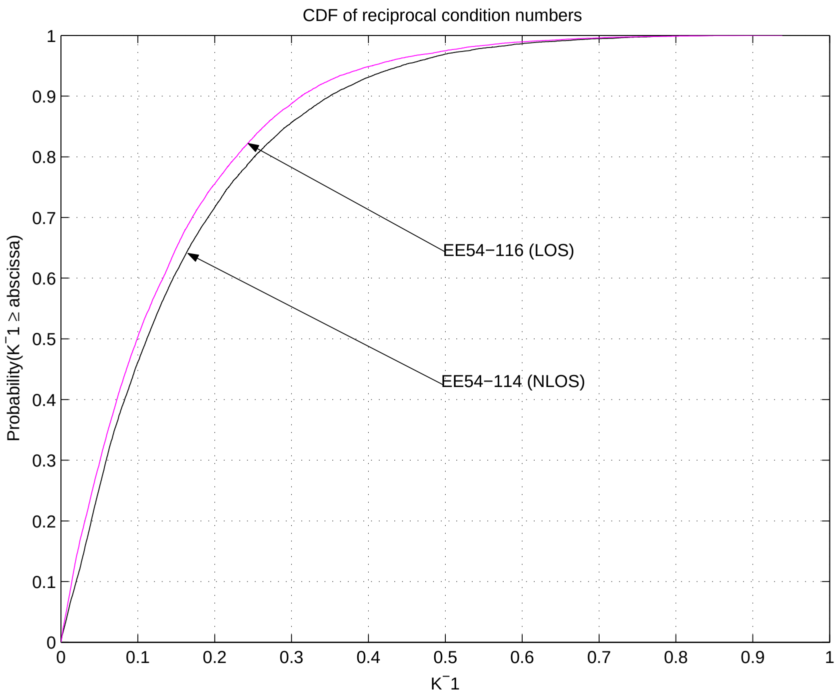

The channel matrix ***H*** is an *N*x*M* matrix with rank *R*.
M = num of transmit antennas
N = num of receive antennas
ρ_R = Received *SNR*,
ε_k = singular values of ***H***

Reciprocal condition number

$$K^{-1} = \frac{\min(\varepsilon_k)}{\max(\varepsilon_k)}$$

Capacity curves in EE54-114

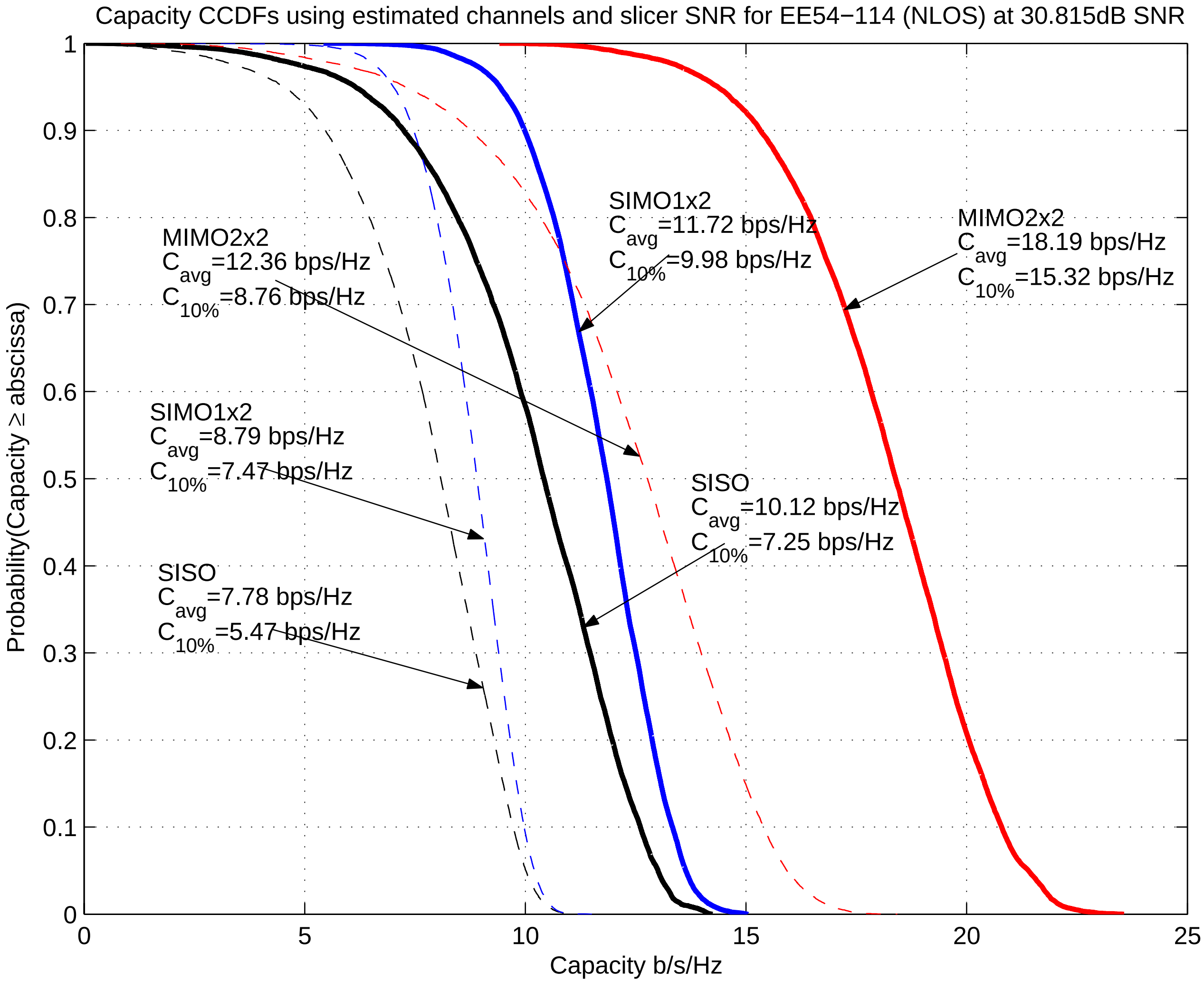

Keep received power Constant for all cases By referring back to the Tx.

Theoretical channel Capacity:

$$C = \log_2(\det(I_M + \frac{\rho_R}{M} H^H H)$$

Capacity measured using slicer SNR

$$C_{slicer} = \log_2(1 + SNRout)$$

Optimizing Overhead Using Capacity

10 symbols	15 symbols	25 symbols	35 symbols
13.15%	19.73%	32.89%	46.05%

5 pilot subcarriers	10 pilot subcarriers	20 pilot subcarriers
2.4%	4.8%	9.7%

Average capacity using slicer SNR

10 training 20 pilots	151.27 Mbps
15 training 20 pilots	144.34 Mbps
25 training 20 pilots	123.09 Mbps
35 training 20 pilots	99.36 Mbps

5 pilots 25 training	130.39 Mbps
10 pilots 25 training	128.52 Mbps
20 pilots 25 training	123.09 Mbps

10 training 5 pilots	157.66 Mbps

RELIC – An 8x8 MIMO Detection ASIC for Wideband MIMO-OFDM System

Major Challenges for RELIC

- Wideband MIMO with high antenna count
  - Up to 8x8, 25MHz bandwidth
- Dynamic reconfiguration for
  - Different number of antennas
  - Different antenna configurations
  - Different FFT sizes
- Highly flexible packet structure support
  - including UCLA METEOR, IEEE 802.11a/g/n

Wideband MIMO up to 8x8

- Algorithm research
  - RLS algorithm offers MMSE performance, fast convergence, and automatic adaptation to various channel conditions
- Implementation friendly architecture
  - Systolic array RLS algorithms and architectures
- Frequency domain scalability
  - Full band mode (25MHz) up to 4x4 and half band mode up to 8x8 (12.5MHz)
- Linear interpolation in frequency domain to reduce hardware complexity

Support for Different Packet Types

- Innovative input tagging scheme
  - Supports different packet structures including UCLA METEOR and IEEE802.11a/g/n
- Real-time reconfiguration of packet structure parameters such as
  - Length of packet
  - Number of OFDM subcarriers
  - Length of training and retraining sequences

Design Process of RELIC

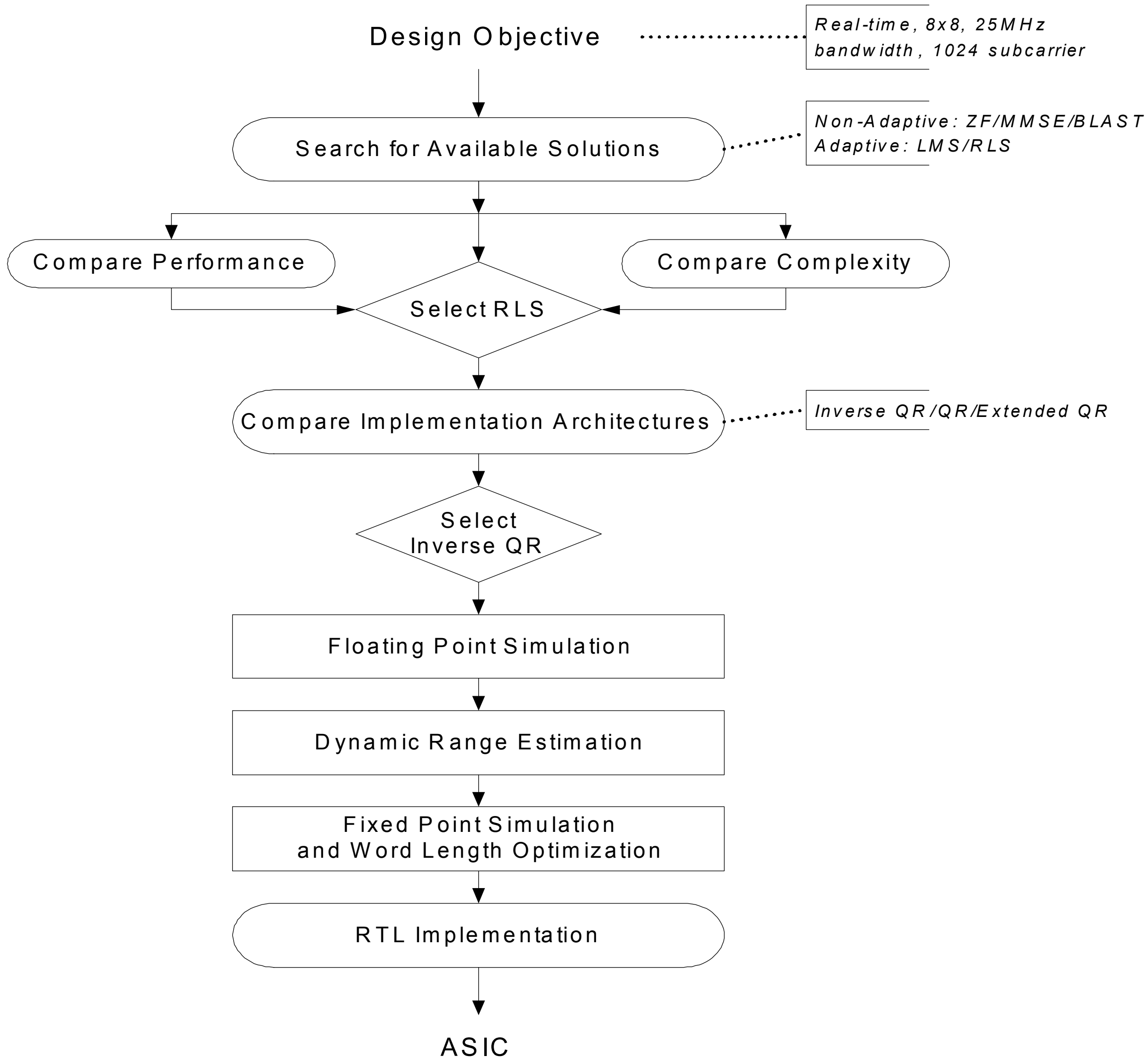

Simulation Results – MMSE vs. MMSE-VBLAST

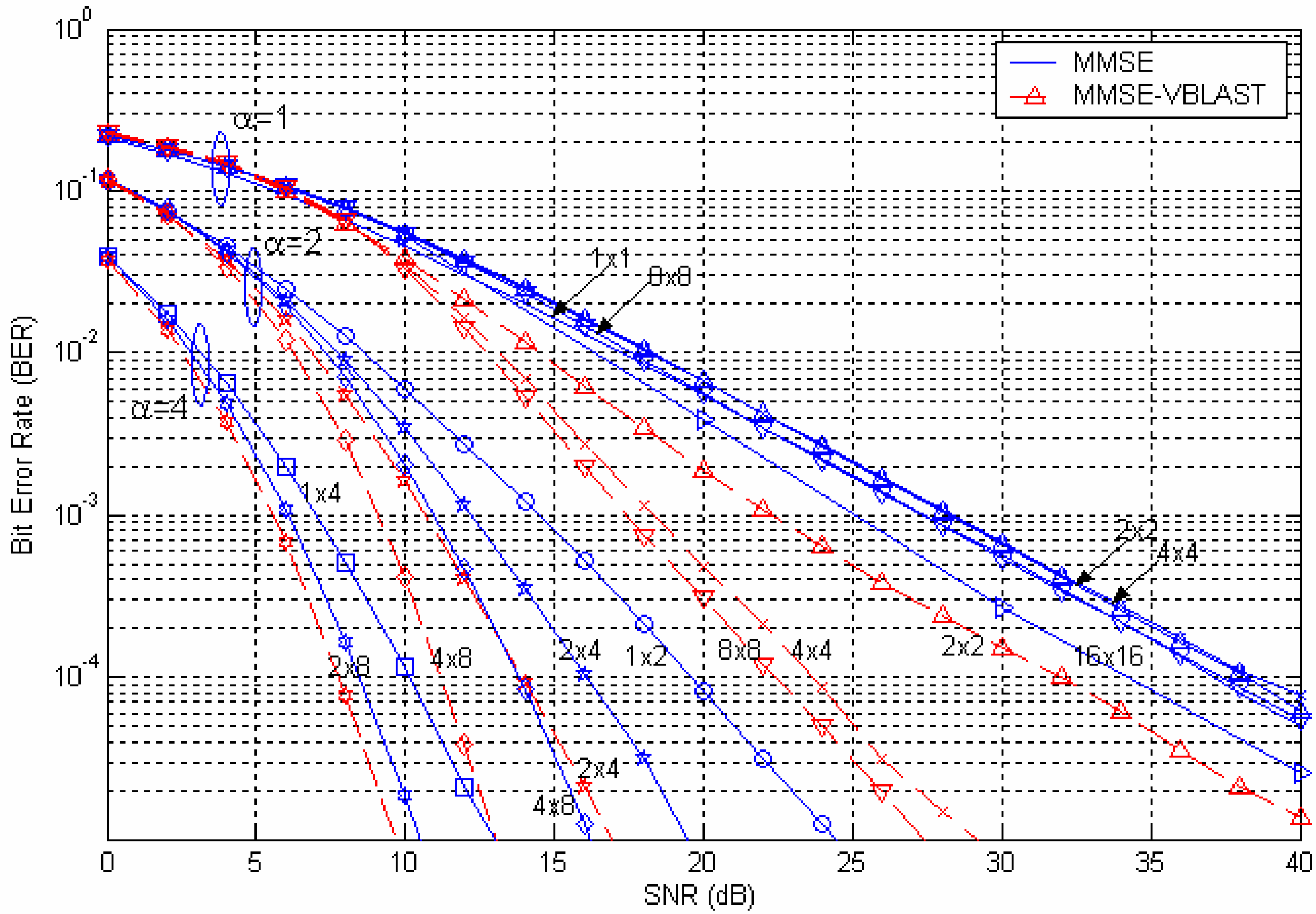

Simulation Results – MMSE vs. ZF-VBLAST

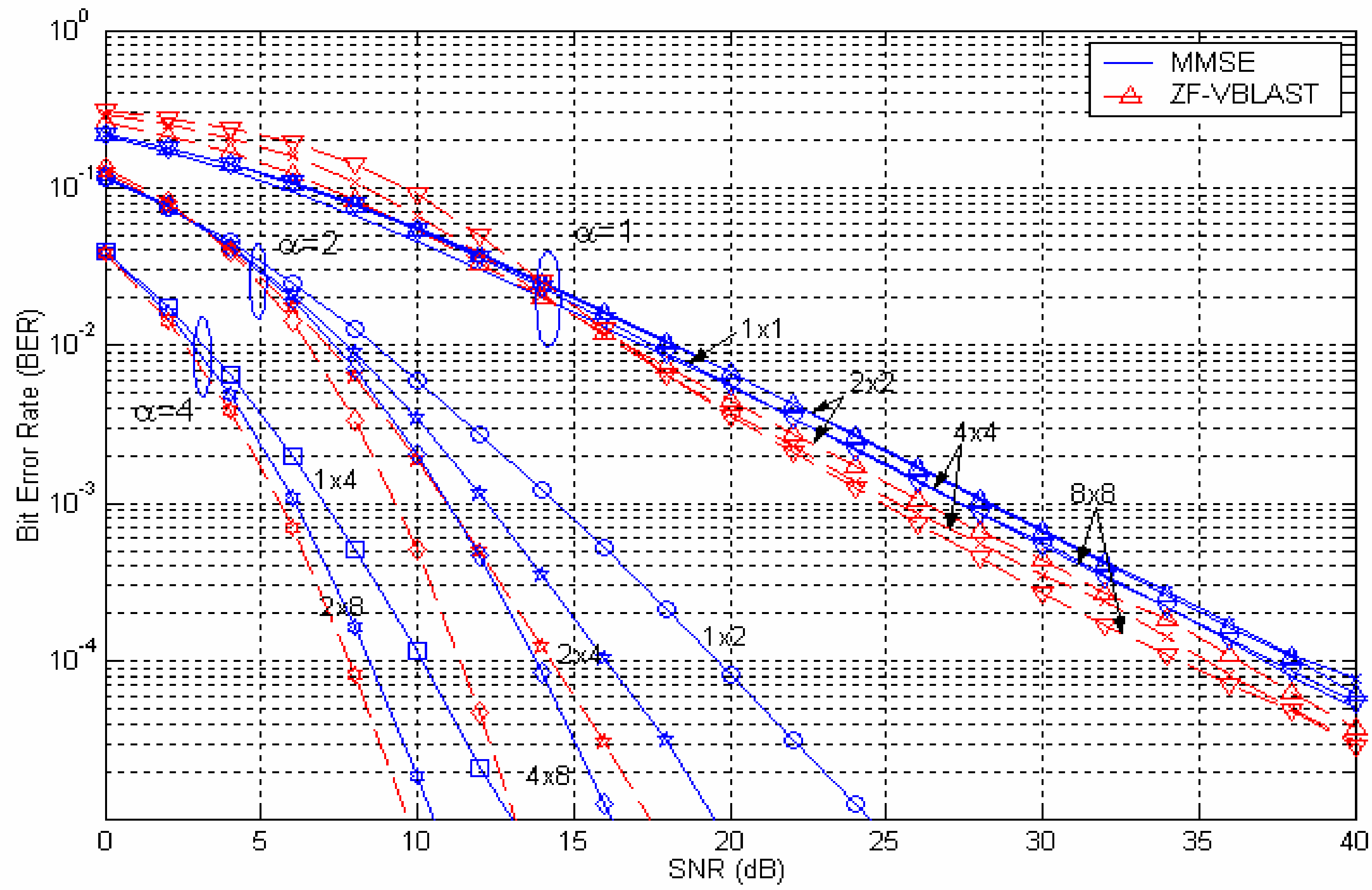

Required SNR (dB) for Uncoded BER=10^{-3} (QPSK)

Nt×Nr	***ZF***	***MMSE***	***ZF-VBLAST***	***MMSE-VBLAST***
1×1	27.4	27.4	27.4	27.4
2×2	**29.9**	**28.2**	**25.4**	**18.3**
4×4	**33.1**	**28.3**	**25.4**	**18.3**
8×8	36.0	27.3	24.8	17.4
1×2	14.4	14.4	14.4	14.4
2×4	**12.5**	**12.2**	**11.0**	**10.7**
4×8	11.4	11.0	9.3	9.1
1×4	7.0	7.0	7.0	7.0
2×8	6.2	6.1	5.6	6.5

Channel RMS Delay Spread vs. Interpolation (Nc=256, 1x1)

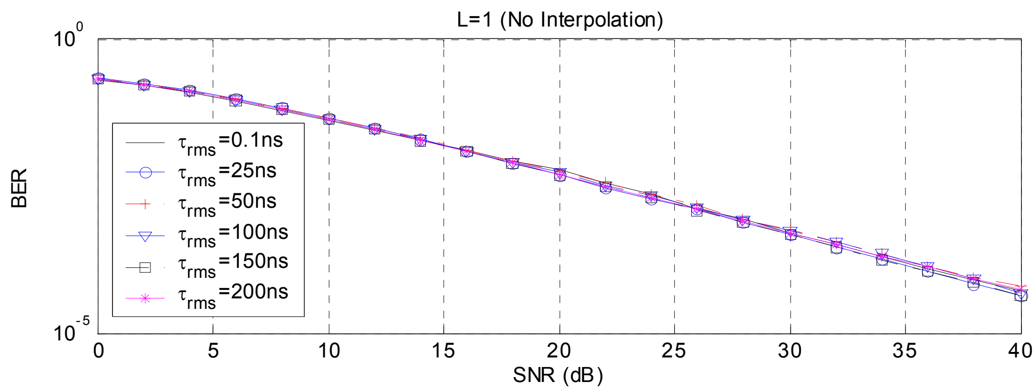

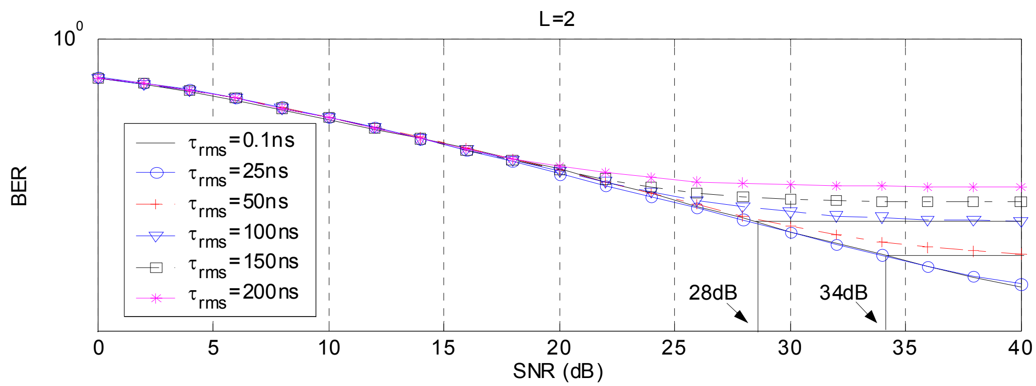

- When L=1, the BER floor in N_c=64 case has disappeared because the cyclic prefix length is sufficiently long (2560ns for N_c=256)
- When L=2, the floor is:
  - @τ_{rms}=50ns: SNR_{max}=34dB, BER_{min}=0.02%,
  - @τ_{rms}=100ns: SNR_{max}=28dB, BER_{min}=0.07%

A Fully Pipelined Inverse QR-RLS Architecture for OFDM

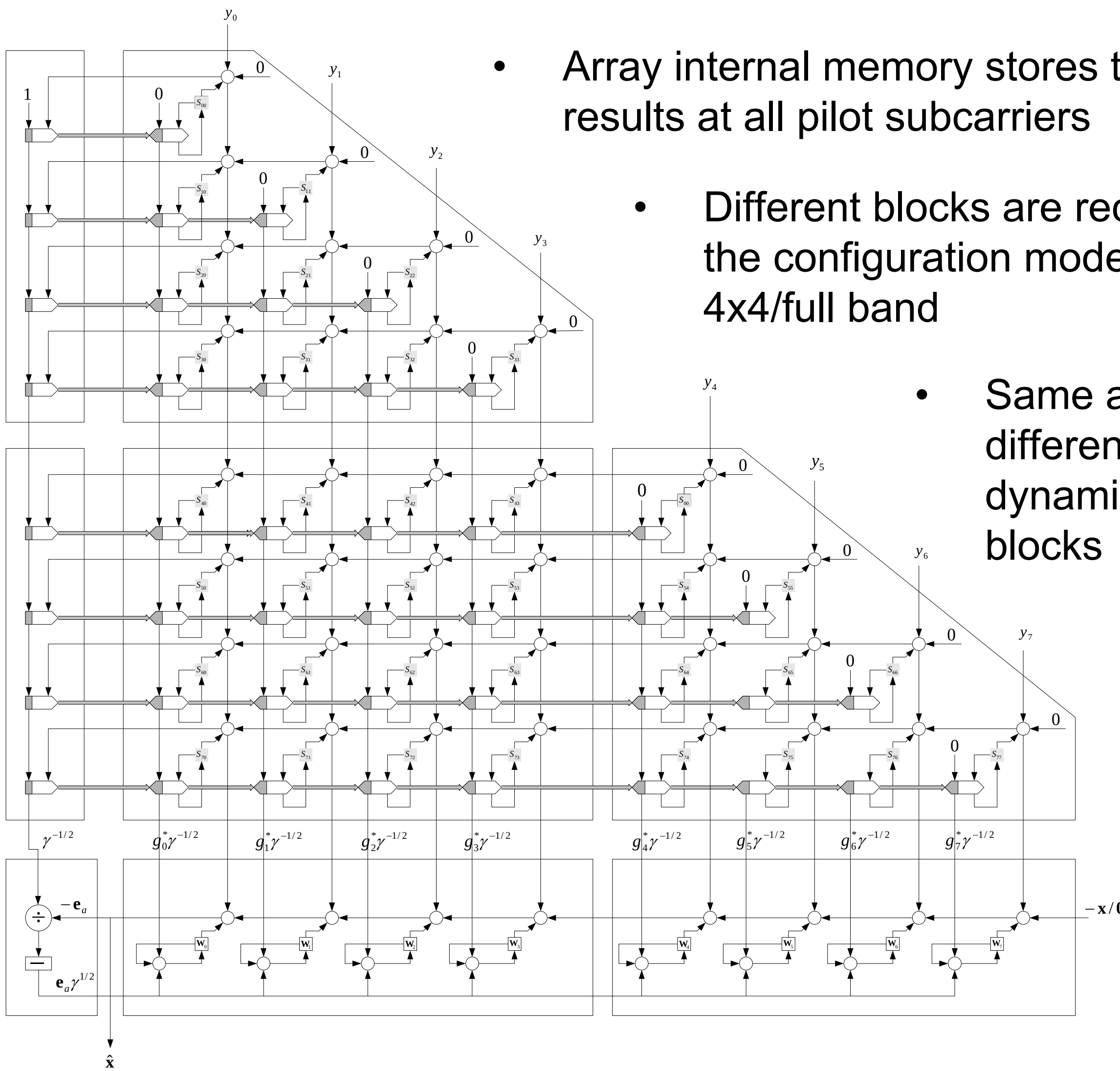

- Array internal memory stores the QR decomposition results at all pilot subcarriers
  - Different blocks are reconnected according to the configuration mode, i.e. 8x8/half band, or 4x4/full band
    - Same architecture supports all different antenna setups by dynamically connecting different blocks
      - Combining array has been mapped onto a linear array by timing multiplexing

Topology of Different Configuration

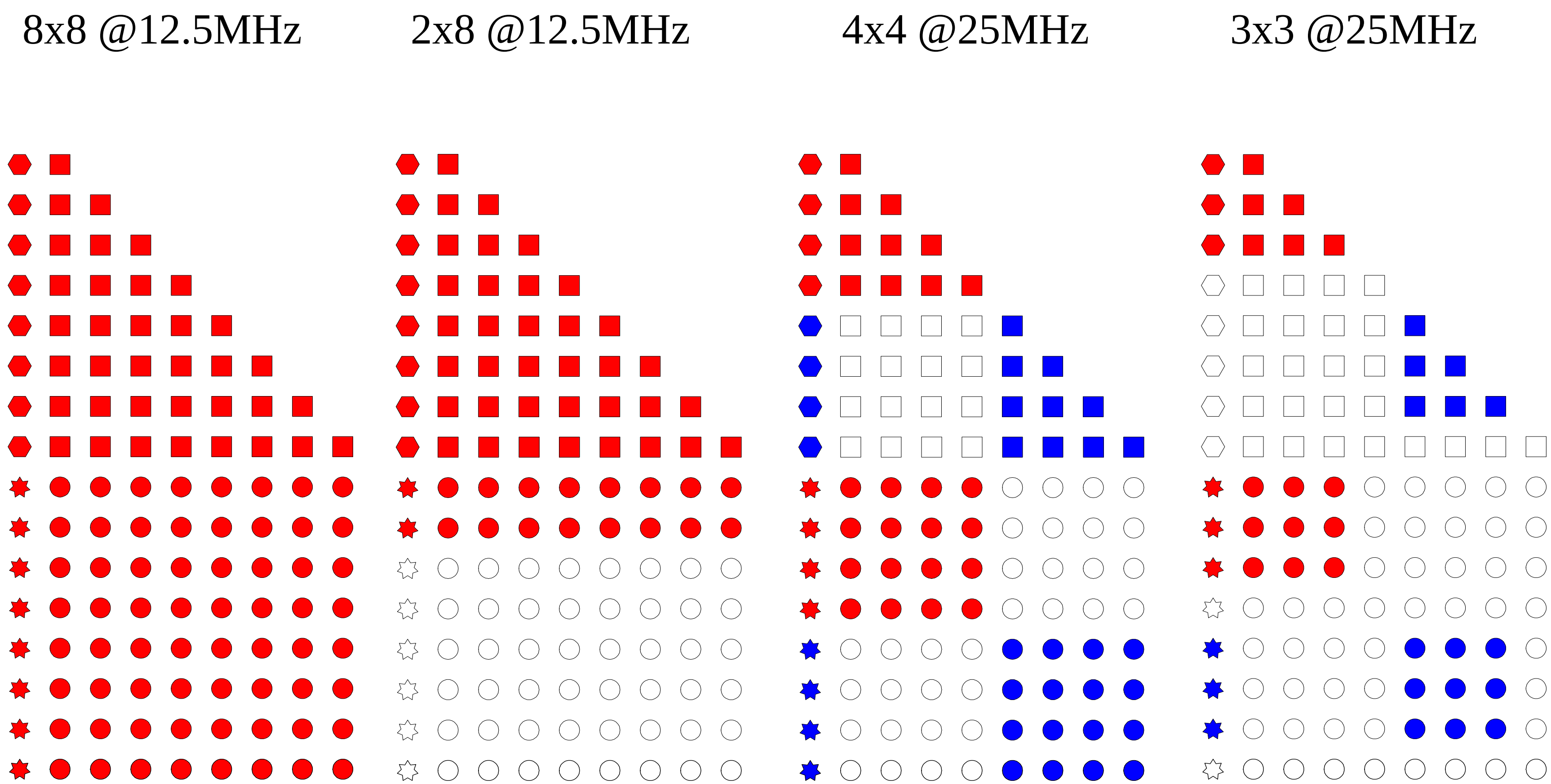

RELIC Specifications

- Maximum clock frequency: 50 MHz
- Supported antenna setup: any valid combination of antennas (Nt≤Nr) up to 8x8
- Dual modes
  - Full band (25MHz): up to 4x4 with 1024 subcarriers
  - Half band (12.5MHz): up to 8x8 with 512 subcarriers and expandable to full band with two RELIC chips
- Real-time (packet-wise reconfigurable) receive antenna selection (soft switching)
- Extremely flexible architecture that can be easily adapted to different OFDM packet structures

RELIC Die Microphotogragh

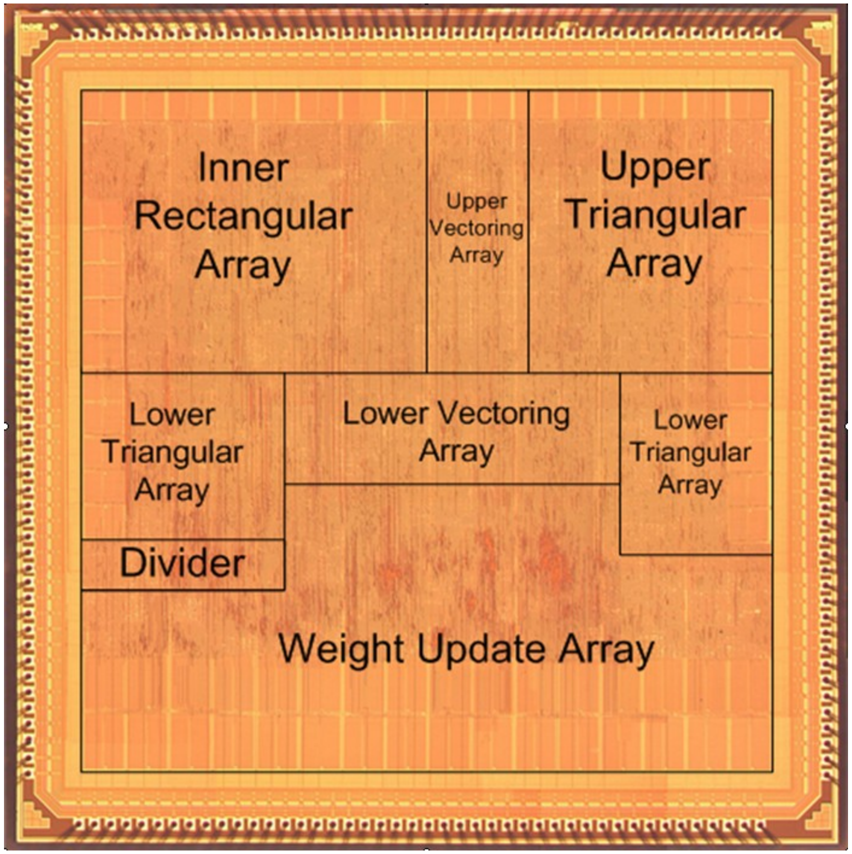

- Process: TSMC 0.18um CMOS, 3.3V/1.8V
- Die Size: 39.4mm^2 (core: 29.2mm^2)
- Gate Count: 2.3M (SRAM: 819Kb)
- Packaging: 181-lead PGA
- Power: 360mW (@58MHz, 2x2)
- Clock Freq: 50MHz (max: 58MHz)